DICER^{HET} PRIMARY NEURONAL CULTURE MODEL FOR STUDYING ROLE OF miRNA BIOGENESIS PATHWAY IN PARKINSON'S DISEASE

Shirin Soleimanbeigi
Master's thesis
University of Helsinki
Faculty of Agriculture and Forestry
Biotechnology

July 2020

HELSINGIN YLIOPISTO
HELSINGFORS UNIVERSITET
UNIVERSITY OF HELSINKI

Tiedekunta – Fakultet – Faculty Faculty of Agriculture and Forestry		Koulutusohjelma – Utbildningsprogram – Degree Programme Biotechnology
Tekijä – Författare – Author Shirin Soleimanbeigi		
Työn nimi – Arbetets titel – Title *Dicer*^{HET} primary neuronal culture model for studying role of miRNA biogenesis pathway in Parkinson's disease		
Oppiaine/Opintosuunta – Läroämne/Studieinriktning – Subject/Study track Biotechnology		
Työn laji – Arbetets art – Level Master's thesis	Aika – Datum – Month and year July 2020	Sivumäärä – Sidoantal – Number of pages 74

Tiivistelmä – Referat – Abstract

Selective degeneration and dysregulation of specific neuronal populations is a common hallmark shared by neurodegenerative diseases affecting the aging population. Parkinson's disease (PD) is one of the most prevalent neurodegenerative diseases with debilitating clinical manifestations that follow a chronic and progressive course. Pathological hallmarks of PD involve gradual and specific loss of DA (DA) neurons and widespread presence of Lewy body (LB) inclusions that consist of aggregated presynaptic protein, α-Synuclein (αSyn). Treatment of PD remains to be at symptomatic management as the underlying mechanisms that trigger neurodegeneration are still not fully elucidated.

Over the past two decades, microRNAs (miRNAs) have become a major area of interest within biomedical fields and gained increasing momentum in the context of neurodegenerative diseases. In recent developments, changes in mature miRNA profiles have been reported in aging tissue and many age-related diseases, including PD. More recently, a number of studies have found that the most essential enzyme in the miRNA biogenesis pathway, *Dicer*, exhibits reduced expression with aging. To these ends, a genetic mouse model based on heterozygous knockout of *Dicer* (*Dicer*^{HET}) was introduced to simulate *Dicer* downregulation. Initial investigations identified the *Dicer*^{HET} model as a promising tool for studying the relationship between disrupted miRNA biogenesis and neurodegeneration associated with PD. To facilitate future investigations and speed up screening of potential therapeutic compounds using this genetic model, in the current work, we aimed to produce a *Dicer*^{HET} *in vitro* model with a practical and convenient genetic engineering approach. The main focus of this work was to validate the model and establish a standardized reproducible approach suitable for research that addresses the role of miRNA biogenesis in PD.

The desired *Dicer*^{HET} genotype was generated *in vitro* by employing traditional *Cre/loxP* system in conjunction with a virally mediated Cre expression. More specifically, primary cortical cultures, derived from *Dicer*$^{flox/+}$ mice embryos, were transduced with Cre expressing lentiviral vectors (lenti-hSYN-T2A-Cre) to delete the "floxed" *Dicer* allele. To establish optimal parameters for the procedure, we analysed recombination efficiency under different transduction conditions. The most efficient recombination was achieved after 5 days of induction in cultures. However, we observed that *Dicer*^{HET} genotype did not attenuate survival of the cells, as assessed by immunohistochemistry. Further, as a proof of concept, we exposed the *Dicer*^{HET} cultures to pre-formed fibrils (PFFs) - a PD related stressor that causes αSyn aggregation. pSer129-αSyn-positive LB-like aggregates were detected in all the PFF-treated cultures, however, with a greater accumulation in the *Dicer*^{HET} cultures. Interestingly, increased aggregation was not accompanied by increased cell death, suggesting that *Dicer*^{HET} genotype does not increase vulnerability of cortical neurons to pSer129-αSyn aggregation. Based on our earlier studies we presume that DA neurons may bear a specific vulnerability towards the age-related Dicer depletion. More conclusive evidence on this intriguing relationship could be provided in future research using the *Dicer*^{HET} model that can be readily applied to primary DA cultures.

Avainsanat – Nyckelord – Keywords
Dicer, microRNA, Parkinson's disease, *Cre/loxP*, lentiviral vectors, preformed fibrils, PFF, Lewy body

Ohjaaja tai ohjaajat – Handledare – Supervisor or supervisors
Andrii Domanskyi (Ph.D., Docent), Piotr Chmielarz (Ph.D.) and Teemu Teeri (Prof.)

Säilytyspaikka – Förvaringställe – Where deposited
Faculty of Agriculture and Forestry

Muita tietoja – Övriga uppgifter – Additional information

HELSINGIN YLIOPISTO
HELSINGFORS UNIVERSITET
UNIVERSITY OF HELSINKI

Tiedekunta – Fakultet – Faculty Maatalous-metsätieteellinen tiedekunta	Koulutusohjelma – Utbildingsprogram – Degree Programme Biotekniikka	
Tekijä – Författare – Author Shirin Soleimanbeigi		
Työn nimi – Arbetets titel – Title *Dicer*^{HET} primäärinen hermosoluviljemämalli miRNA-biogeneesireitin roolin tutkimiseksi Parkinsonin taudissa		
Oppiaine/Opintosuunta – Läroämne/Studieinriktning – Subject/Study track Biotekniikka		
Työn laji – Arbetets art – Level Pro Gradu -tutkielma	Aika – Datum – Month and year Heinäkuu 2020	Sivumäärä – Sidoantal – Number of pages 74

Tiivistelmä – Referat – Abstract

Tiettyjen hermosoluryhmien vajaatoiminta ja rappeutuminen on ikään liittyville hermoston rappeumasairauksille yhteinen ilmentymä. Parkinsonin tauti (PD) on yleinen etenevä hermoston rappeumasairaus, jonka oireet pahenevat taudin edetessä. Tautia luonnehtii dopamiinia (DA) tuottavien hermosolujen asteittainen rappeutuminen sekä merkittävät proteiinikertymälöydökset, ns. Lewyn kappaleet (Lewy body; LB), jotka koostuvat lähinnä presynaptisesta proteiinista nimeltä α-synukleiini (αSyn). PD:n hoitoratkaisut painottuvat edelleen oireiden lievitykseen, sillä hermorappeumaa käynnistäviä tautimekanismeja ei vielä täysin ymmärretä.

Kahden edellisen vuosikymmenen aikana mikroRNA (miRNA)-molekyylit ovat herättäneet suurta kiinnostusta eri biolääketieteen aloilla ja saaneet erityistä huomiota hermorappeumasairauksien tutkimuksessa. Viimeisimmät kehitykset viittaavat siihen, että miRNA-tasot muuttuvat sekä ikääntymiskudoksessa että monien ikään liittyvien sairauksien yhteydessä, kuten PD:ssä. Tuoreissa tutkimuksissa on myös havaittu, että Dicer:in, miRNA-molekyylien synteesireitin tärkeimmän entsyymin, ilmentyminen alentuu ikääntymisen myötä. Tätä mekanismia on pyritty jäljittelemään *Dicer*^{HET} hiirimallilla, joka perustuu *Dicer*-geenin heterotsygoottiseen mutageneesiin. Alustavissa tutkimuksissa *Dicer*^{HET}-malli osoittautui lupaavaksi tutkimusmalliksi häiriintyneen miRNA-synteesireitin ja PD:hen liittyvän hermorappeuman välisen yhteyden tutkimiseen. Täten, tulevien tutkimustöiden helpottamiseksi ja lääkeaineseulontojen nopeuttamiseksi, tässä työssä olemme pyrkineet tuottamaan vastaavaa *Dicer*^{HET} *in vitro* mallia soveltamalla kätevää perimänmuokkauksen menetelmää. Tavoitteena oli kelpuuttaa malli ja luoda yhdenmukainen ja toistettava menetelmä tuleviin töihin, joissa tutkitaan miRNA-biosynteesin roolia PD:n tautimekanismissa.

Dicer^{HET}-genotyyppi tuotettiin soluviljelmissä, yhdistämällä perinteistä *Cre/loxP*-systeemiä viruksen välittämään Cre-synteesiin. Tarkemmin ottaen, aivokuoren primääriviljelmät, jotka olivat peräisin *Dicer* $^{flox/+}$ -hiirien alkioista, transdusoitiin Cre:tä ilmentävillä lentivirusvektoreilla (lenti-hSYN-T2A-Cre) "*loxp*-rajatun" *Dicer*-alleelin poistamiseksi. Määrittääksemme menetelmälle optimaaliset parametrit, arvioimme rekombinaatiotehokkuutta eri transduktio-olosuhteissa. Optimaalisissa olosuhteissa pystyimme saavuttamaan tehokkaan rekombinaation 5 päivän induktion jälkeen viljelmissä. Immunohistokemialliset värjäykset osoittivat kuitenkin, että *Dicer*^{HET} -genotyyppi ei heikentänyt solujen eloonjäämistä. Havainnollistaaksemme tutkimusmallin konseptia, altistimme *Dicer*^{HET}-viljelmät vielä ns. ennalta muodostetuille fibrilleille (pre-formed fibrils; PFF) – tämä on PD:een liittyvä stressitekijä, joka saa αSyn-proteiinit kertymään rykelmiin. pSer129-αSyn-positiivisia LB:n kaltaisia rykelmiä havaittiin kaikissa PFF-käsitellyissä viljelmissä. Rykelmiä kertyi kuitenkin enemmän *Dicer*^{HET}-viljelmiin. Tämä ei kuitenkaan aiheuttanut lisääntynyttä solukuolemaa, mikä viittaa siihen, että *Dicer*^{HET} -genotyyppi ei lisää aivokuoren neuronien haavoittuvuutta pSer129-αSyn-kertymiä kohtaan. Aikaisempien tutkimuksiemme perusteella oletamme, että DA-hermosolut ovat erityisen herkkiä ikääntymiseen liittyvää Dicer-entsyymitason alentumista kohtaan. Tästä kiehtovasta yhteydestä olisi mahdollista saada lisänäyttöä tulevissa tutkimuksissa soveltamalla *Dicer*^{HET}- mallia yhtä helposti primäärisiin DA-neuroneihin.

Avainsanat – Nyckelord – Keywords
Dicer, mikroRNA, Parkinsonin tauti, *Cre/loxP*, lentivirusvektori, ennalta muodostetut fibrillit, PFF, Lewyn kappale

Ohjaaja tai ohjaajat – Handledare – Supervisor or supervisors
Andrii Domanskyi (FT, Dosentti), Piotr Chmielarz (FT) and Teemu Teeri (Prof.)

Säilytyspaikka – Förvaringställe – Where deposited
Maatalous-metsätieteellinen tiedekunta

Muita tietoja – Övriga uppgifter – Additional information

Table of Contents

1 Introduction 8

2 Review of literature 9

2.1 Parkinson's disease 9

2.2 miRNA biogenesis pathway and Parkinson's disease 12

2.2.1 miRNAs 12

2.2.2 Biogenesis of miRNAs 16

2.2.3 Dicer 18

2.2.4 Models based on *Dicer* ablation 20

2.2.5 Conditional *Dicer* knockout models 21

2.2.6 Inducible *Dicer* deletion in adult mice 25

2.2.7 *Dicer* ^{HET} model 26

3 Aims of the study 27

4 Materials and Methods 27

4.1 Human cell culture 27

4.2 Lentiviral production and concentration procedures 28

4.2.1 Isolation of vectors from bacterial stocks 29

4.2.2 Preparation of packaging cells 30

4.2.3 PEI stocks 30

4.2.4 PEI-mediated transient transfection 30

4.2.5 Viral collection and concentration 31

4.3 Heterozygous *Dicer* knockout in primary neuronal cultures 31

4.3.1 Mouse strains 31

4.3.2 Preparation of cortical primary neuron cultures 32

4.3.3 Lentiviral transduction 34

4.3.4 PFF treatment 34

4.4 Genotyping 35

4.4.1 DNA extraction 35

4.4.2 PCR amplification 35

4.4.3 Agarose gel electrophoresis (AGE) 36

4.5 Western blot 37

4.5.1 Lysis of cortical neurons 37

4.5.2 sodium dodecyl sulphate-polyacrylamide gel electrophoresis (SDS-PAGE) 37
4.5.3 Membrane transfer and immunodetection 38
4.6 Quantitative reverse transcription PCR (RT-qPCR) 39
4.6.1 RNA extraction 39
4.6.2 Reverse transcription (RT) 40
4.6.3 Quantitative PCR (qPCR) 40
4.7 Immunofluorescent staining 41
4.8 Automated high throughput microscopy and data analysis 42
4.8.1 Automated high throughput microscopy 42
4.8.2 Image processing and segmentation 42
4.8.3 Data analysis 43

5 Results 44

5.1 Generation of *DICER^{HET}* mouse primary cortical cultures 44
5.1.1 Gene editing efficiency 45
5.1.2 Investigation of transcript and protein levels 49
5.2 Effects of heterozygous *Dicer* ablation on pathologic αSyn propagation 50
5.2.1 Assessing vulnerability of *Dicer^{HET}* primary cortical neurons 51
5.2.2 αSyn aggregation may be increased in *Dicer^{HET}* primary cortical cultures 52

6 Discussion 55

6.1 Validation of the *Dicer^{HET}* model 55
6.2 Studying αSyn propagation in the *Dicer^{HET}* model 56

7 Conclusions 58

8 Acknowledgments 59

9 References 60

ABBREVIATIONS

AGE – agarose gel electrophoresis

AGO – argonaute

ANOVA – analysis of variance

bp – base pair

BSA – bovine serum albumin

cDNA - complementary DNA

CKO – conditional knockout

CNS – central nervous system

DA – dopamine

DAPI – 4',6-diamidino-2-phenylindole

Dat – dopamine transporter

DIV – days *in vitro*

DMEM - Dulbecco's Modified Eagle's medium

DPBS – Dulbecco's Phosphate-Buffered Saline

dsRNA – double stranded RNA

E. coli - Escherichia coli

EDTA - Ethylenediaminetetraacetic acid

FBS – fetal bovine serum

Floxed - flanked by *loxP*

GFP - green fluorescent protein

HBSS – Hank's balance salt solution

HEK293T – human embryonic kidney 293 cells

kDA – kilodalton

KO – knockout

LB – Lewy body

L-dopa – levodopa

LN – Lewy neurite

LvV – lentiviral vector

miRNA – microRNA

mRNA – messenger RNA

ncRNA– non-coding RNA

ND – neurodegenerative disease

NeuN – neuronal nuclei

PBS – phosphate-buffered saline

PCR – polymerase chain reaction

PD – Parkinson's disease

PEI – polyethylenimine

PFA – Paraformaldehyde

PFFs – preformed fibrils

pre-miRNA – precursor microRNA

pri-miRNA – primary microRNA

qPCR – quantitative polymerase chain reaction

pSer129-αSyn – phosphorylated αSyn at residue Ser129

RISC – RNA-induced silencing complex

RNAi – RNA interference

RNAse – ribonuclease

ROS – reactive oxidative species

RT – reverse transcription

RT-qPCR – quantitative reverse transcription polymerase chain reaction

SD – standard deviation

SDS-PAGE – sodium dodecyl sulfate-polyacrylamide gel electrophoresis

Ser129 – serine 129

siRNAs – small interfering RNAs

SN – substantia nigra

SNpc – substantia nigra pars compacta

TAE – tris acetate-EDTA

VTA – ventral tegmental area

WB – western blot

αSyn – α-synuclein

1 Introduction

Parkinson's disease (PD) is a common age-associated neurodegenerative disease characterized by gradual loss of dopamine (DA) neurons and widespread deposits of aggregated protein called α-synuclein (αSyn) (Dauer & Przedborski 2003). Current treatments of PD remain focused on symptomatic management as the underlying mechanisms that trigger neurodegeneration are still unknown. In recent years, there have been increasing interest in deciphering the role of non-coding RNAs (ncRNAs) in the pathogenesis of human diseases. Proliferation of studies in the field of RNA during the past two decades has revealed that microRNAs (miRNAs) have a conserved role in many common human diseases, ranging from cardiovascular diseases to various cancers and neurodegenerative diseases (NDs) (Zhang, 2008; Maciotta et al., 2013; Rupaimoole and Slack, 2017). This association is also well recognized in PD and is supported by numerous empirical studies that have linked aberrant miRNA expression to PD pathology (Kim et al., 2007; Cuellar et al., 2008; Pang et al., 2014; Chmielarz et al., 2017).

miRNAs are small (~20 nt) regulatory RNAs that mediate one of the three pathways of RNA interference (RNAi) (Wilson and Doudna 2013). They regulate gene expression at a post-transcriptional level by targeting mRNAs. miRNA networks play a prominent part during development of nervous system and survival and maintenance of DA neurons during aging (Sontag 2010; O'Carroll and Schaefer 2013). Changes in mature miRNA profiles have been detected in aging tissue and many serious age-related diseases, suggesting that decreased miRNA levels may be a contributing factor in their development (Kim et al., 2007; Gehrke et al., 2010; Dimmeler and Nicotera, 2013). Reduced miRNA profiles may be a consequence of a decreased expression of miRNAs or a disrupted miRNA biogenesis pathway due to age-associated decreased expression of its most essential enzyme, Dicer (Schaefer et al., 2007, Chan and Kocerha, 2012). Indeed, data from several sources suggest that Dicer levels decline along with miRNAs in aging tissue and in aging related diseases (Simunovic et al., 2010; Mori et al., 2012; Boon et al., 2013; Emde et al., 2015; Chmielarz et al., 2017).

In view of the recent developments and important insights into the role of miRNAs as crucial regulators, in particular, in the central nervous system (CNS), further efforts exploring their role in pathogenic processes are necessary as they may offer a better understanding of underlying pathological mechanisms and reveal novel therapeutic agents. Dicer has long been a major focus within the field of miRNAs. Knockout studies that alter Dicer activity, have been at the heart of understanding miRNAs' significance and their functions and targets (Radhakrishnan and Alwin, 2016). Recently, in a study conducted by our group, it was shown that heterozygous knockout of the *Dicer* gene (termed $Dicer^{HET}$) results in downregulation of number of different miRNAs and to cause PD-like symptoms in the animals (Chmielarz et al., 2017). It was also shown that a Dicer activating compound, enoxacin, promoted survival of the $Dicer^{HET}$ DA neurons in culture. Even though enoxacin is not an ideal drug as a Dicer enhancer for *in vivo* use, this example highlights Dicer enhancing agents as promising candidates in neuroprotection. Therefore, in this thesis project, it was of interest to establish a $Dicer^{HET}$ *in vitro* model that could be utilized in further studies as a platform for initial drug screening and for unravelling the role of miRNA biogenesis pathway in neurodegeneration.

In particular, in this project, we aimed to produce and establish a $Dicer^{HET}$ *in vitro* model by applying a gene-editing method that combines *Cre/loxP* recombination system with viral gene delivery. The theoretical dimensions of the project are laid out in the next chapter, which provides a brief review of PD, examines the emerging role of miRNAs in pathology and reviews several relevant *Dicer* knockout studies. Due to practical constraints, a comprehensive review of individual miRNAs has not been provided in this thesis.

2 Review of literature

2.1 Parkinson's disease

Parkinson's disease (PD) is a chronic and relentlessly progressive neurodegenerative disease (ND) that is affecting 1% of individuals older than 60 years and reaches 4% at the age of 80 years (de Lau and Breteler, 2006). It is the most common form of movement disorder and after Alzheimer's disease, the second most common ND (de Lau and Breteler, 2006).

Old age is the predominant risk factor for developing PD, regardless of ethnicity or geographical location (Driver et al., 2009; Collier et al., 2011). However, gender and cross-cultural variations exist, with higher predisposition being reported among men and in Europe, North America and South America (Kalia and Lang, 2015; Moisan et al., 2016). Globally, the prevalence of PD continues to increase as a result of aging population and remarkably prolonged life expectancy in both developed and undeveloped countries (United Nations, 2015, The 2015 Revision of World Population Prospects). The number of individuals affected by PD doubled between 1990 to 2016, from 2.5 million to 6.2 million, alongside the rising proportion of elderly in the population (GBD 2016 Parkinson's Disease Collaborators, 2016). Accordingly, it is projected (conservatively) that by 2050 the global prevalence of the disease will rise to atleast 12 million patients (GBD 2016 Parkinson's Disease Collaborators, 2016). Needless to say, that such increase in prevalence will impose a progressively increasing societal and economic burden, which e.g. currently in the US has a financial impact of $51.9 billion annually for 1 million affected patients (The Lewin group, 2019, Economic Burden and Future Impact of Parkinson's Disease: Final Report).

PD is characterized by gradual and specific loss of pigmented dopamine (DA) neurons in the substantia nigra pars compacta (SNpc) region of basal ganglia (Dauer and Przedborski, 2003). Another key pathological hallmark of PD includes aberrant presence of intracellular inclusions and filaments called Lewy bodies (LBs) and Lewy neurites (LNs), respectively. These structures are proteinaceous deposits and are mainly comprised of misfolded and aggregated presynaptic protein α-synuclein (αSyn) and other associated proteins (Spillantini et al., 1997; Goker-Alpan et al., 2010). Degeneration of DA neurons leads to DA depletion and dysfunction in the dorsal striatum, which has a key role in refining and controlling motor movement (Guttman et al., 1997; Hornykiewicz, 1998). The disease is usually diagnosed upon appearance of first physical signs, by the time when approximately 50-80% of the DA neurons have been already lost (Bernheimer et al., 1973; Riederer and Wuketich, 1976). Diagnostic features of PD comprise three “cardinal” motor symptoms - rigidity, bradykinesia and rest tremor - and a wide range of debilitating non-motor symptoms, some of which precede the onset of cardinal motor symptoms by decades and may have a more detrimental impact on quality of life (Schrag et al., 2000; Chaudhuri et al., 2006). The non-motor symptoms are possibly caused by disturbances and spreading neurodegeneration and LB formation in cholinergic, noradrenergic, and serotonergic systems, and they include

neuropsychiatric disorders, such as sleep disturbances, anxiety and depression, autonomic disabilities such as constipation and fatigue, sensory disturbances, such as hallucinations and loss of smell and other miscellaneous symptoms (Chaudhuri et al., 2006; Klingelhoefer et al., 2017).

The etiology of PD largely remains elusive. At the present PD is considered to be a complex multifactorial disease with variable contributions from genetic, epigenetic and environmental factors (Ascherio and Schwarzschild, 2016; van Heesbeen and Smidt, 2019). Majority of PD cases (95%) however have a sporadic component with an unknown cause (idiopathic PD) (Di Monte et al., 2002; Warner and Schapira, 2003; Cannon and Greenamyre, 2013). Environmental factors contributing to the onset of the disease can range from exposure to certain toxins or diets to head injuries and bacterial and viral infections (Ascherio and Schwarzschild, 2016). The familial cases of PD account for 5-10% of patients and they have been traced to a number of different mutations with autosomal dominant or recessive Mendelian inheritance mechanisms (Lill, 2016). The first causative gene was discovered in 1997 when a missense mutation in αSyn gene (SNCA) was reported to cause familial autosomal dominant PD (Polymeropoulos et al., 1997). To date, several other mutations of SNCA gene have been linked to PD/parkinsonism and mutations in a number of other protein coding genes involved in different molecular pathways have been identified with monogenic or polygenic influence on the PD phenotype (Anderson et al., 2006; Kumar et al., 2011). Interestingly, PD phenotypes in both sporadic and familial cases of the disease are often indistinguishable from each other and they may for that reason share the same pathogenic molecular pathways (Baba et al., 2006; Papapetropoulos et al., 2007). Common denominator implicated in both forms of the disease is a profound degeneration of nigrostriatal DA neurons, but a conclusive concept has not yet been built to explain the biochemical events that trigger and feed this process. Accumulation of misfolded αSyn aggregates, endoplasmic reticulum stress, mitochondrial dysfunction, accumulation of reactive oxidative species (ROS) and other toxic metabolites, altered proteasome and autophagy functions and neuroinflammation - all which have been frequently associated with the disease process, may act alone or more likely in an elaborate interplay with such and other yet uncovered factors (Mercado et al., 2013; Segura-Aguilar et al., 2014; Ransohoff, 2016; Ambaw et al., 2018; Chen et al., 2019b). Currently, advancing age is recognized as the biggest risk factor for developing PD (Collier et al., 2011). Many biochemical alterations seen in PD, such as genomic instability, mitochondrial dysfunction

and neuroinflammation are also involved in the normal process of aging (Ransohoff, 2016; Surmeier et al., 2017; Poewe et al., 2017). Combination of many such adverse changes that accompany aging may particularly affect DA neurons due to their distinct functional and metabolic needs (Sulzer et al., 2007). Therefore, studying the molecular pathways that are affected as a consequence of normal aging may very likely provide important insights into compromised DA neuron viability associated with PD (Rodriguez et al., 2015).

As molecular mechanisms of pathogenesis in PD is complicated and chronological order of biochemical events that compromise DA neuron viability remains obscure, to date there is yet no causal treatment for the disease. The standard treatment remains to be based on DA replacement therapy (DA precursors and DA agonists), which alleviates the motor symptoms by compensating for the depleted striatal DA levels (PD Med Collaborative Group, 2014; LeWitt et al., 2016). Over the last 50 years, the leading therapy for PD has been the prodrug levodopa (L-dopa), which is a DA precursor that can pass the blood-brain barrier and enter the CNS where the enzyme DOPA decarboxylase converts it to DA, hence restoring the nigrostriatal DA neurotransmission (LeWitt et al., 2016). Despite of its therapeutic advantages, L-dopa treats the disease symptoms with variable efficiency, does not treat the non-motor symptoms, has considerable side effects and 5-10 years after initiation of the therapy loses its effect in most patients, while causing more debilitating motor symptoms than the disease itself (Chaudhuri et al., 2018). In advanced stages of the disease, when the benefits of the medication are undermined by the side effects and drug induced complications, deep brain stimulation therapy (requires surgical implantation) can be used as a last resort to alleviate the motor symptoms (Fox et al., 2011; Fasano et al., 2012). However, benefits of this technique are limited to selected patients with idiopathic forms of PD and like the medication it cannot halt nor reverse the evolution of the disease - that is enigmatic progressive neuronal death (Shih and Tarsy, 2007; Fox et al., 2011).

2.2 miRNA biogenesis pathway and Parkinson's disease

2.2.1 miRNAs

MicroRNAs (miRNAs) are small regulatory molecules, from the large class of non-coding RNAs (ncRNAs) (Carthew and Sontheimer, 2009). They regulate gene expression at post-transcriptional level by inducing degradation and/or transcriptional repression of target

mRNA transcripts synthesized from endogenous genes. Post-transcriptional gene regulation was not discovered until the turn of the century when the first miRNAs were described. The first miRNA was identified in 1993 by the joint efforts of Lee et al., (1993) and Wightman et al., (1993). They reported of finding a 22 nt long non-protein coding transcript, lin-4, in *Caenorhabditis elegans,* which they had discovered to have antisense complementarity to 3' UTR region in lin-14 mRNA. They found that due to this complementarity, lin-4 could bind to lin-14 mRNA, and subsequently result in decreased expression of lin-14 protein, without any changes in lin-14 mRNA levels. Second miRNA was described 7 years later, in 2000, upon reports of finding a 21 nt long let-7 transcript that was involved in *C. elegans* development (Reinhart et al., 2000; Slack et al., 2000). This transcript however was discovered to be conserved across species; homologues of let-7 were detected in vertebrates, ascidians, hemichordates, mollusks, annelids and arthropods (Pasquinelli et al., 2000; Lagos-Quintana et al., 2001). After this finding, the two examples described over the course of a decade, challenged the prevailing central dogma of cellular biology, and triggered an explosion in research efforts solely dedicated to search for new small ncRNAs. Now, nearly two decades later thousands of miRNAs with diverse functions have been identified in different species, and details regarding their general mechanisms, such as biogenic processes and post-transcriptional repression mechanisms, have been elucidated (Melo and Melo, 2014; de Rie et al., 2017; Kozomara et al., 2019). Currently, miRBase database (www.mirbase.org), the main miRNA online repository that collects annotated information on published miRNAs, lists 38589 hairpin precursor miRNA sequences from 271 species (Griffiths-Jones, 2004; Griffiths-Jones et al., 2008). Of these, 2654 mature miRNAs processed from 1917 precursor miRNAs are listed for humans and 1978 mature miRNAs processed from 1234 precursor miRNAs are listed for mice. New miRNAs still continue to be identified and new breakthroughs in experimental methods emerge every year (de Rie et al., 2017; Chen et al., 2019a).

Today, it is well-recognized that miRNAs exert myriad regulatory roles in essential cellular functions across all species (Bartel, 2004; Carthew and Sontheimer, 2009; Mendell et al., 2012; Sherrard et al., 2017). They form complex highly dynamic regulatory networks, which have a critical role during animal development, neuronal development being no exception to this (Fu et al., 2013; Nowakowski et al., 2018). In humans, miRNAs may regulate more than half of all protein coding genes (Friedman et al., 2009). They orchestrate embryonic development and further continue to be tightly involved in tissue growth and maintenance

and remain as essential regulators of varied biological functions (Dogini et al., 2014; Cho et al., 2019). Although intracellular gene regulation is the primary function of miRNAs, they also contribute to cell communication by acting as intercellular signaling molecules (O'Brien et al., 2018). miRNAs are therefore also found outside the cells in bodily fluids, where they are referred to as circulating miRNAs (Weber et al., 2010). miRNAs can be also released in circulation as a result of apoptosis, tissue damage and necrosis (Kai et al., 2018). Not surprisingly, aberrant miRNA profiles have been observed in correlation with many pathological conditions (Schaefer et al., 2007; Gehrke et al., 2010; Hébert et al., 2010; Cao et al., 2016).

Studies such as that conducted by Landgraf et al., (2007) have revealed that in normal physiological conditions miRNAs exhibit cell- and tissue-specific expression patterns. These distinct miRNA profiles seem often to be altered in diseased tissue (Ikeda et al., 2007; Lukiw, 2007; Zhang, 2008; Gardiner et al., 2012; Ahmadinejad et al., 2017; Kanno et al., 2017; Lu et al., 2017). On this ground, extracellular miRNAs have been proposed by a large and growing body of studies as potential biomarkers (Hayes et al., 2014; Wang et al., 2016a; Huang, 2017). Changes in mature miRNA profiles have been reported to be associated with many serious diseases, particularly in cancer where miRNA levels are for the most part decreased (Lu et al., 2005; Esteller, 2011; Tufekci et al., 2014; Lin and Gregory, 2015; Bracken et al., 2016; Paul et al., 2018). In cancer, it is also well known that miRNAs have tumor suppressor and oncogenic activity and are involved in tumor progression (Deng et al., 2008; Palanichamy and Rao, 2014). Moreover, a considerable literature has been published on miRNAs specific cancer associated patterns, which hold a promise to revolutionize diagnostic, therapeutic and prognostic procedures (Calin et al., 2006; Lan et al., 2015). Indeed, there has been also a growing interest in screening miRNAs for potential prognostic markers of PD and other NDs (Mushtaq et al., 2016). For example, expression of miR-103a-3p, miR-30b-5p and miR-29a-3p is specifically observed to be dysregulated in PD, making them relevant choices for biomarkers (Serafin et al., 2015). Increasingly growing data on miRNA signatures could be eventually useful for early and accurate non-invasive diagnosis and for following the disease state (Mushtaq et al., 2016).

Approximately 70% of the miRNAs discovered do date have been found to be present in the central nervous system (de Pietri Tonelli et al., 2014). Interestingly however, only a

subset of miRNAs is enriched in the brain (Landgraf et al., 2007; Sethi and Lukiw, 2009; Lukiw, 2012), where they are expressed and distributed differentially depending on brain region, cell type and even cellular compartment (Smirnova et al., 2005; He et al., 2007; Kye et al., 2007). More fascinatingly, a number of miRNAs are synthesized in synaptic areas such as dendrites, axons and dendritic spines, where they locally control synaptic function, shape synapse morphology and contribute to learning and memory (Hu and Li, 2017). Moreover, many of brain enriched miRNAs interact with disease related genes in PD (Goh et al., 2019). miRNA profiling of brain samples from diagnosed PD-patients have revealed dysregulation of several individual miRNAs, some of which are involved in αSyn-mediated neurotoxicity, mitochondrial dysfunction and oxidative stress and neuroinflammation (Miñones-Moyano et al., 2011; Alvarez-Erviti et al., 2013; Prajapati et al., 2015; Slota et al., 2019). Discussion on individual miRNAs implicated in PD lies beyond the scope of this literature review. This subject is extensively reviewed elsewhere (Goh et al., 2019).

miRNA profiling studies have generated many leads to follow in the future. At the moment, despite of ongoing research efforts, miRNAs role in PD still remains poorly defined. Moreover, technical limitations and lack of standardized protocols have contributed to many inconsistencies between the reported observations (Roser et al., 2018). Hence, much work still remains to be done before findings on miRNAs can be translated into therapeutic gains. However, it has been already unequivocally established that miRNAs play a prominent part during development of nervous system and survival and maintenance of neurons during aging (Davis et al., 2015; Chmielarz et al., 2017). Much of this information have come from investigations that have altered global miRNA levels by disturbing function of Dicer, which is an essential enzyme involved in miRNA biogenesis (Grishok et al., 2001). Indeed, there is also evidence that Dicer levels, along with global miRNA levels, are dysregulated during aging and in age-related diseases, such as in PD and amyotrophic lateral sclerosis (ALS) (Simunovic et al., 2010; Mori et al., 2012; Dimmeler et al., 2013; Emde et al., 2015; Chmielarz et al., 2017). As aging is considered the greatest risk factor for PD, it could be argued that altered miRNA function could ultimately underlie the multiple molecular and cellular processes implicated in PD. miRNA biogenesis pathway will be described in the next section and *Dicer* knockout studies will be discussed further in the later sections.

2.2.2 Biogenesis of miRNAs

In humans, a significant percentage of miRNA genes are intragenic, meaning that they reside within previously annotated protein coding regions (host genes), and are mostly processed from introns (Hinske et al., 2010; Hinske et al., 2014). The rest are intergenic and form transcription units (TUs) where they are transcribed from their own promoters as long primary transcripts (named pri-miRNAs) (Kim and Kim, 2007; de Rie et al., 2017). A large portion of the pri-miRNAs consist of clusters of different miRNAs, which are often related to each other and participate in common pathways (Berezikov, 2011; Wang et al., 2016b). Related miRNAs bear similarities in their seed regions (nucleotides 2-8 at the 5'-end), which also serves as a basis for dividing miRNAs into different families (Thatcher et al., 2008; Bartel et al., 2009).

Mature and functional miRNAs arise through multiple processing events that takes place both in the nucleus and the cytoplasm (Figure 1). Most of miRNAs are transcribed by RNA polymerase II and regulated by RNA Pol II-associated transcription factors and epigenetic regulators (Lee et al. 2002; Lee et al., 2004a; Chuang and Jones, 2007). The transcription products are >1000 nt long pri-mRNA transcripts that get capped at the 5' end and polyadenylated at the 3' end (Cai et al., 2004; Lee et al., 2004a). The mature miRNA sequences reside within the local stem loop structures. Following transcription, pri-mRNA molecules are subjected to a stepwise trimming process that eventually results in ~20 nt long functional miRNAs (Lee et al., 2002). First step in miRNA maturation process takes place in the nucleus where the primary transcripts are cleaved into shorter hairpin-shaped precursors, called precursor miRNAs (pre-miRNAs) (Lee et al., 2003). This step is carried out by the microprocessor complex, which comprise a type III RNAse, Drosha, and its essential cofactor DiGeorge syndrome critical region 8 (DGCR8) (Gregory et al., 2004). pre-miRNA hairpins are then exported by Ran-GTP/Exportin 5 dependent mechanism to the cytoplasm where the maturation process can be completed (Yi et al., 2003; Lund et al., 2004). In the cytoplasm pre-miRNA-molecules are further cleaved by a Drosha homologue, Dicer, to yield duplex miRNAs of 19–25 nt (Grishok et al., 2001; Ketting et al., 2001). With additional aid from Dicer and TAR RNA-binding protein (TRBP) protein, one of the double stranded RNA (dsRNA) strands are selected to bound to an Argonaute (AGO) protein (Kobayashi et al., 2016). This results in the formation of mature RNA-induced silencing complex (RISC) that goes on to find its targets based on

Watson Crick base pairing between the seed region located on the 5' end of the selected guide single stranded RNA (ssRNA) and the miRNA-recognition element [MRE]) in the 3' UTR region of the target mRNA (Bartel 2009; Ha and Kim, 2014).

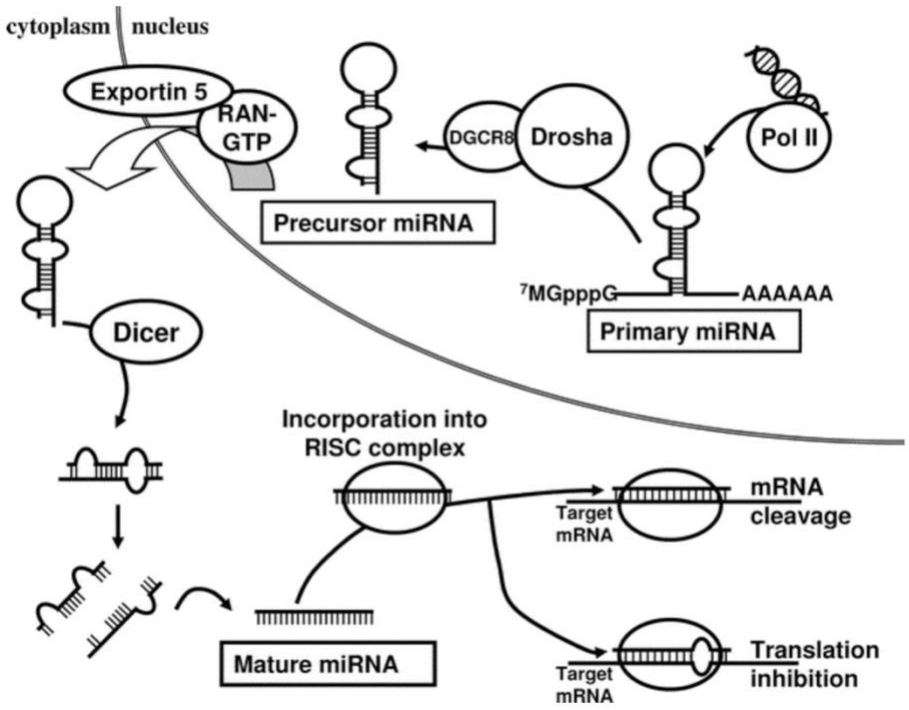

Figure 1 Canonical miRNA biogenesis pathway. Following polymerase II (Pol II) mediated transcription, hairpin-shaped primary miRNAs (pri-miRNAs) are subjected to a stepwise trimming process. The first step is catalyzed in the nucleus and mediated by the microprocessor complex (Drosha–DiGeorge syndrome critical region 8 (DGCR8)). The products, precursor miRNAs (pre-miRNAs), are then exported into the cytoplasm by Exportin 5 and its GTP-binding cofactor Ran (Ran-GTP). In the cytoplasm pre-miRNAs associate with a cytoplasmic complex that includes the Dicer enzyme. pre-miRNAs are further cleaved and processed into mature single stranded miRNAs that incorporate into RISC complex to guide translational repression. Figure reprinted from Chuang and Jones (2007).

Interaction of miRNAs with the targets can result in translation repression, mRNA destabilization or rarely in AGO-catalyzed degradation of the target mRNA (Selbach et al., 2008; Uhlmann et al., 2012). Since each single miRNA may have hundreds of targets, they

can affect expression of one or possibly hundreds of proteins, or even entire cellular pathways. Moreover, miRNAs can also interact with other regions in their target mRNAs, such as 5'UTR regions, coding sequences and promoters, adding to the complexity of their function (Broughton et al., 2016). Thus, not surprisingly, miRNAs can regulate hundreds of genes, including those of other miRNAs or genes involved in miRNA biogenesis pathway while each gene can be regulated by hundreds of miRNAs (Selbach et al., 2008; Uhlmann et al., 2012).

2.2.3 Dicer

As was discussed earlier, the endoribonuclease activity of Dicer has a pivotal role in the maturation process of most miRNA molecules. Dicer was initially identified in 2001, shortly after Nobel winning discovery of RNAi (Fire et al., 1998; Bernstein et al., 2001). It was described as a member of ribonuclease (RNAse) III family of enzymes that show catalytic specificity to dsRNA and produces consistently short ~22 nucleotide RNA fragments (Bernstein et al., 2001). As yet, Dicer has transpired to be a ubiquitous enzyme. It is present in most eukaryotic organisms with RNAi mechanism and constitutes of a highly conserved protein architecture across species (Cerutti and Casas-Mollano, 2006; Shabalina and Koonin, 2008). A number of duplicates have however emerged during evolution and interestingly some species mediate processing of small RNAs by employing more than one Dicer paralog (Murphy et al., 2008; de Jong et al., 2009). For example, plants express four nuclear Dicer homologues, DCL1–4, of which the DCL-1 is responsible for miRNA processing while the rest are taking part in anti-viral defense (Hiraguri et al., 2005; Xie et al., 2005; Blevins et al., 2006). Insects, such as *Drosophila melanogaster* express two different Dicer paralogs, DCR-1 and DCR-2, of which former accounts for processing miRNAs and latter for processing small interfering RNAs (siRNAs) (Lee et al., 2004b). In mammals, in contrast, biogenesis of both miRNAs and siRNAs are mediated with one cytoplasmic Dicer protein, encoded from a single large multi-exonic gene (*DICER1* in *Homo sapiens* and *Dicer1* in *Mus musculus;* referred to with the alias name *Dicer* throughout this work) (Carthew and Sontheimer, 2009; De jong di et al., 2009; Svobodova et al., 2016).

Dicer is a multi-domain protein (Figure 2). Mammalian Dicers are very large enzymes with molecular mass of ~220 kDA (Billy et al., 2001; Provost et al., 2002; Kotaja et al., 2006;

Much et al., 2016). Dicers of lower eukaryotes are often smaller and have less complicated domain structures. However the metazoan and plant Dicers share atleast the following common structural features: An N-terminal ATPase/helicase domain, a domain of unknown function (DUF-283), a PAZ (Piwi/Argonaute/Zwille) domain, two RNAse III domains (RNAse IIIa and RNAse IIIb) and a C-terminal dsRNA binding domain (dsRBDs) (MacRae et al., 2006; Weinberg et al., 2011; Doyle et al., 2012). The active site of the protein resides in the interface of two RNAse domains that form an intramolecular dimer (Zhang et al., 2004; MacRae et al., 2007). Because metazoan Dicers are very large proteins, their crystal structures have not yet been solved. Crystallographic structural information of an intact Dicer has so far been based on a small 82 kDA Dicer from the protozoan *Giardia intestinalis;* presented in Figure 2 (MacRae et al., 2006). Although a homolog, the *Giardia* Dicer lacks atleast the helicase, dsRBDs and DUF-283 domains which are present in higher eukaryotic Dicers, such as in humans (Figure 2).

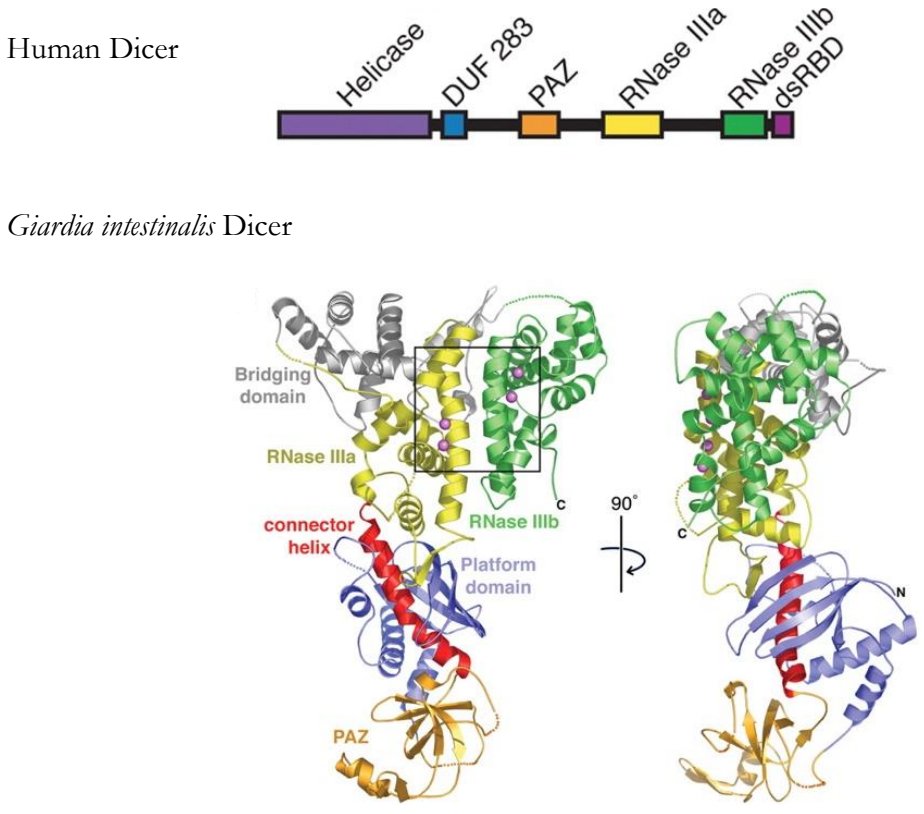

Figure 2 Schematic representation of a typical eukaryotic Dicer enzyme. Above, the primary sequence of human Dicer, which is comprised of a helicase domain, a domain of unknown function (DUF-283), a PAZ (Piwi/Argonaute/Zwille) domain, two RNAse III

(RNAse IIIa and RNAse IIIb) domains and a dsRNA binding domain (dsRBDs). The ribbon diagrams below show the crystal structure of *Giardia intestinalis* Dicer which serves as a comparative model for Dicer in higher eukaryotes. The left figure shows the front view and the right figure shows the side view. As seen, the *Giardia* Dicer lacks some of the characteristic domains present in Dicer of higher eukaryotes. Reprinted from MacRae et al. (2006).

By prevailing perception, Dicer is a cytoplasmic endoribonuclease specialized in miRNA processing and along with Drosha are indispensable enzymes for this process. However, this view is being reshaped in light of growing reports that implicate Dicer in various functions beyond the canonical RNAi pathway (Burger & Gullerova, 2015; Song & Rossi, 2017). For instance, in one study it was shown that *Dicer* deletion in retinal pigment epithelium of mice induces a phenotype that mimics symptoms of age-related macular degeneration (Kaneko et al., 2011). Interestingly, this phenotype was absent in mice lacking other crucial proteins of RNAi pathway, such as Drosha, suggesting an RNAi independent mechanism by which Dicer contributes to retinal health. Furthermore, functional Dicer have been found to be present in exosomes and in the nucleus, where it associates with various nuclear proteins (Burger & Gullerova, 2015; Song & Rossi, 2017). Some of emerging non-canonical activities of Dicer include participation in autophagy, DNA damage response, transcriptional silencing and viral defense. In agreement with these activities, Dicer promotes tolerance to stress. In the other hand, Dicer expression and activity is itself repressed under adverse cellular and environmental conditions, such as oxidative stress, ultraviolet (UV) radiation and hypoxia, which in turn weakens stress tolerance (Mori, et al. 2012; Emde & Hornstein, 2014). As cellular stress is the hallmark of aging and correlates with various pathologies, it is not a coincidence that aberrant Dicer expression is observed in many human disorders and conditions such as cancer, NDs and even in psychiatric conditions such as depression, posttraumatic stress disorder and schizophrenia (Simunovic et al., 2010; Sanders et al., 2013; Wingo et al., 2015).

2.2.4 Models based on *Dicer* ablation

As Dicer activity has a prominent importance in maturation process of nearly all vertebrate miRNAs, an easy way to determine collective role of miRNAs is to genetically ablate Dicer. Several such knockout studies were conducted shortly after discovery of the enzyme, and they provided compelling evidence that Dicer has a vital role in vertebrate development

(Bernstein et al., 2003; Wienholds et al., 2003; Giraldez et al., 2005). First study to demonstrate this, showed that zygotic knockout of the *Dicer* gene, by disrupting the exon 21 that directly impacts catalytic activity of the second RNase III domain, results in arrest of embryogenesis by embryonic day 7.5 (E7.5) (Bernstein et al., 2003). Another similar study, in which Yang et al., (2005) generated a strong hypomorphic mutation in mice zygotes by deleting exons 1 and 2, embryos died between E12.5 and E14.5, while also displaying severe defects in angiogenesis. Consistently, corresponding *Dicer* knockout studies in zebrafish also provided similar results from a developmental perspective (Wienholds et al., 2003; Giraldez et al., 2005). Giraldez et al., (2005) also reported of defected brain morphogenesis, which for the first time provided insight into the role of miRNAs in CNS development (Giraldez et al., 2005). Together, these studies indicated that prenatal Dicer ablation forestalls normal early development and can have embryonically lethal consequences.

2.2.5 Conditional *Dicer* knockout models

As discussed, Dicer has a vital role in the early development. In order to study the role of miRNAs in later development, it is imperative to use conditional knockout strategies to circumvent the early embryonic lethality of the *Dicer* null genotype (Bernstein et al., 2003; Harfe et al., 2005). Accordingly, numerous conditional knockout models (CKO), which allow temporal and spatial gene deletion, have been generated during various studies (Radhakrishnan and Alwin, 2016). These models have made a significant contribution to understanding of miRNA mediated gene regulation in vertebrates and the role of miRNAs in the CNS development and function.

One of the most widely used approaches to generate a *Dicer* CKO has been by employing *Cre/loxP* system (Radhakrishnan and Alwin, 2016). In brief, *Cre/loxP* is a recombination system derived from bacteriophage P1, where 38 kDA recombinase protein Cre catalyzes site-specific DNA deletion between two *loxP* sequences (Sternberg and Hamilton, 1981; Sternberg et al., 1986; Sauer, 1998). Each *loxP* site is a 34 bp consensus sequence consisting of two 13 bp long inverted and palindromic repeat sequences that flank an 8 bp core sequence. DNA excision is carried out from the 8 bp core sequences (Nagy, 2000). Generally, *Cre/loxP* animals are produced by crossbreeding two separately generated transgenic animal strains, which are referred to as Cre driver strain and floxed strain. Cre

driver strain contains the Cre recombinase expressing transgene and floxed strain contains the two requisite *loxP* sites that flank a critical sequence in the targeted gene (Sauer and Henderson, 1988; Tsien et al., 1996). As floxed gene is present in all the cells of the transgenic animal, the spatial specificity of gene deletion is controlled by predetermining the expression site for Cre recombinase (Tsien et al., 1996). Typically, this is done by placing *Cre* transgene under a tissue or cell specific promoter. Moreover, by choosing a promoter that is activated during a specific developmental stage or upon introduction of an external stimulus, it is also possible to control timing of the gene deletion (Nagy, 2000; Zhuang et al., 2005; McLellan et al., 2017). However, such spatiotemporal control of Cre expression is possible only with the condition that suitable promoters are available. An alternative method to Cre driver lines is to use recombinant viral vectors for localized expression of Cre recombinase (Sinnayah et al., 2004; Heldt et al., 2007).

What we know about miRNAs role in CNS development is largely based upon empirical studies that utilize *Cre/loxP* system to achieve knockout of *Dicer*. This usually involves breeding *Dicer*$^{flox/flox}$ mice with various forebrain Cre driver mouse strains, such as *Nestin-Cre, Emx1-Cre* or *FoxG1-Cre* (Radhakrishnan and Alwin, 2016). Such systems have allowed us to study the collective role of miRNAs in later stages of development and even in cellular maintenance. For instance, in a pivotal *in vivo* study, Schaefer et al., (2007) employed *Pcp2* promoter-driven Cre recombinase to achieve knockout of *Dicer* in Purkinje cells of the cerebellum of mice. Since *Pcp2* promoter is not activated until the neural cells have differentiated into Purkinje cells (second week from birth), by using this approach, they could ensure that Dicer was not ablated until cells had reached a postmitotic stage. Cre expression upon activation of *Pcp2* promoter lead to ablation of Dicer, which was followed by rapid depletion of cerebellar-expressed miRNAs and progressive degeneration of cerebellum and ataxia *in vivo* (between 13-17 weeks of age). This study not only served as an evidence for importance of miRNAs in neuronal survival and maintenance, but also for the first time argued that Dicer, in correlation with miRNA depletion, may play an important role in neurodegeneration. Following studies were able to address the role of miRNAs in cellular differentiation, function and survival in midbrain (Kim et al., 2007; Huang et al., 2010; Pang et al., 2014), spinal cord (Zheng et al., 2010; Chen and Wichterle, 2012), cerebral cortex (De Pietri Tonelli et al., 2008; Saurat et al., 2013), hippocampus (Li et al., 2011) and retina (Georgi and Reh, 2010). By utilizing different brain-specific genes with different expression patterns it has been possible to assess consequences of Dicer ablation

in a time and neuronal type specific manner. For instance, Cre lines such as *Emx1-Cre* (De Pietri Tonelli et al., 2008; Kawase-Koga et al., 2009), *Nestin-Cre* (Kawase-Koga et al., 2009; McLoughlin et al., 2012; Zindy et al., 2015) and *Foxg1-Cre* (Makeyev et al., 2007; Nowakowski et al., 2011) have been used to determine role of miRNAs in early development of forebrain while *hGFAP-Cre* (Nigro et al., 2012), *CAMKII-Cre* (Davis et al., 2008; Hébert et al., 2010) and *Nex-Cre* (Hong et al., 2013) have been utilized to determine the role of miRNAs in the later development of forebrain.

Most previous studies have consistently reported that *Dicer* deletion leads to severe malformations in the developing tissue, which results in prenatal or early postnatal death of the animals (e.g. Bernstein et al., 2003; Wienholds et al., 2003). To address the effects of *Dicer* deletion at later stages of development, Kim et al., (2007) placed Cre recombinase under control of *DA transporter* (*Dat*) promoter. This promoter is only expressed in midbrain DA neurons and gets activated once the neurons have reached a postmitotic stage. They reported that *Dicer* deletion in mice lead to progressive loss of DA neurons and a PD-like phenotype. By 8 weeks of age 90% of the DA neurons had been lost. This result has been supported by another similar study by Pang et al. (2014), which also reported rapid and progressive loss of DA neurons upon knockout of *Dicer*. In this case *Dicer* deletion was induced in adult DA neurons of ventral tegmental area (VTA) and SNpc by using adeno-associated virus (AAV)-mediated Cre delivery during early postnatal periods (> 8 weeks) (Pang et al., 2014).

It should be pointed out that Dicer ablation studies have not systematically resulted in apoptosis and neurodegeneration. For example, in the above-mentioned study, conducted by Kim et al. (2007), it was also discovered that when *Dicer* was deleted in the murine models, it resulted in nearly 100% loss of DA neurons, whereas only 50% of GABAergic neurons were lost. In another study, Dicer was ablated in dopaminoceptive neurons (basal ganglia) of mice via DA receptor-1 (*Dr-1*) promoter-driven Cre (Cuellar et al., 2008). Predictably Dicer ablated animals displayed characteristic defects associated with loss of miRNAs and dysfunctional DA neurons, such as reduced lifespans, anatomical defects such as reduced brain size, smaller neurons and astriogliosis and several movement defects associated with neurodegeneration. Surprisingly however, despite of confirmed significant loss of miRNAs (miR-124a), no signs of apoptosis or neurodegeneration was detected in the mutated dopaminoceptive neurons.

In summary, majority of the studies have together outlined that there is a plausible connection between Dicer activity and neuronal maintenance and survival. It is also apparent that Dicer (and thus RNAi machinery) has varying roles on cell survival, depending on the tissue type and developmental stages. For example, conditional Dicer ablation in neuroepithelial cells of the hippocampus of mouse, using, *Emx1*-Cre, *Nestin*-Cre and *Nex*-Cre lines, where promoters are activated at either E9.5, E10.5 or E13.5, respectively, have each resulted in specific phenotypes (De Petri Tonelli et al., 2008; Kawase-Koga et al., 2009; Hong et al., 2013). When *Dicer* CKO is generated with the *Emx1-Cre* line, Dicer expression is lost at the onset of neurogenesis and hence it results in severe cortical defects, due to apoptosis and differentiation impairment in hippocampal progenitors (Kawase-Koga et al., 2009; Li et al., 2011). When Dicer is ablated slightly later, by using the *Nestin-Cre* line, progenies also display significantly smaller postnatal cortices, due to altered number of neural progenitors and defects in hippocampal morphology, however to a smaller extent (De Petri Tonelli et al., 2008; Kawase-Koga et al., 2009, Li et al., 2011). *Nex-Cre* (E13.5) assisted *Dicer* deletion, which takes place in postmitotic cells, also causes a reduction in cortex size, but does not affect hippocampal morphology and has a relatively small effect on cell survival (Hong et al., 2013, Li et al., 2011). Indeed, different Cre lines also have different recombination efficiencies (delayed/incomplete *Dicer* deletion), which could have partly accounted for differences in the reported observations (Andersson et al., 2010; Liang et al., 2012). Further complicating this picture are the questions regarding miRNAs turnover rates that can be very slow in some cases (Andersson et al. 2010). Nevertheless, Dicer remains a popular target of manipulation in studies pursuing to unravel the molecular mechanisms of miRNAs. Evidence from the *Dicer* CKO models have provided a glimpse into vast repertoire of miRNAs functions and have argued in favor of their involvement in neurodegenerative diseases. Although Dicer manipulation affects miRNAs functions as a whole, many single miRNAs and targets associated with the *Dicer* knockout phenotype have been identified and manipulation of single miRNAs (or pool of miRNAs) have also been carried out (Kim et al., 2007; Hébert et al., 2010; Peng et al., 2012). In the coming years, rapidly increasing initiatives built on current research coupled with newly emerging genetic and molecular approaches will certainly provide a more holistic understanding of miRNA system and yield new biological insights.

2.2.6 Inducible *Dicer* deletion in adult mice

In addition to the constitutive *Cre/loxP* systems discussed, more advanced *Cre/loxp* systems that get activated in response to external chemical stimuli have also been used successfully to modulate Dicer activity in postnatal brain. Among such strategies CreER^{T2}-Tamoxifen system has gained a wide use. In this system Cre-recombinase is fused to a modified ligand binding domain of the estrogen receptor (ER^{T2}) which can bind a synthetic estrogen analog, Tamoxifen (Feil et al., 1997). Once translated, the fusion protein is bound by heat shock protein 90 (HSP90) and retained in the cytoplasm, preventing the Cre recombinase from acting on its targets. If Tamoxifen is administered, this repression is released upon ligand binding of the receptor domain, granting the CreER^{T2} access to the nuclear compartments where the site-specific recombination takes place. As this system permits a more precise temporal control over recombination, it has allowed to examine effects of Dicer deletion in adult cells and by that contributed in advancing our understanding of biological contexts where miRNAs exert their influence. For example, in a study conducted by Konopka et al. (2010) it was demonstrated that impact of disturbed miRNA processing extends to include neuronal plasticity. As reported, deletion of *Dicer* in forebrain of 8-10-week-old mice, mediated by Tamoxifen inducible *CAMKII-CreER^{T2}*, was accompanied by miRNA depletion and caused a slow neurodegeneration which started at 14 weeks after *Dicer* deletion. However, as pointed out by the authors, degeneration phenotype was relatively modest in comparison with previous studies where *Dicer* deletion using a non-inducible *CAMKII-Cre* system had caused a significant cell death upon birth (Davis et al. 2008). More interestingly, before the onset of neurodegeneration (at 12 weeks after deletion), the *Dicer* null mice displayed an enhanced learning and memory, which was proposed to be linked to observed morphologic changes in dendritic spines and increase in synaptic plasticity proteins such as brain-derived neurotrophic factor (BDNF) and matrix metallopeptidase-9 (MMP-9). These results not only extend earlier studies by highlighting the role of miRNAs on cell survival, but also emphasize that miRNAs impact reaches beyond neural progenitor survival and affect neuronal function at all ages. These findings fit with a recent study published by our group where it was shown that *Dicer* deletion in DA neurons of mice at a postnatal stage also results in neuronal loss (Chmielarz et al., 2017). In this study, *Dicer* deletion was initiated in postmitotic DA neurons (8-10-week-old mice) using the CreER^{T2} recombinase driven by the *Dat* promoter. Early degeneration of DA neurons was noted at 2 weeks following the Tamoxifen injections, which progressed

and eventually resulted in 90 % loss of substantia nigra (SN) DA neurons. Like in PD, DA neuron degeneration was accompanied by increased mitochondrial ROS accumulation and displayed a selective pattern, affecting DA neurons in VTA region to a lower degree. Moreover, neuronal loss caused characteristic PD-like motor manifestations, which was shown to improve by L-dopa administration. To put it differently, it appears that Dicer plays a role in adult DA neuron survival and more notably, SN DA neurons seem to display a selective vulnerability to loss of Dicer function.

2.2.7 *Dicer*^{HET} model

As mentioned above, recently our group extended the studies on *Dicer* mutants and reported that conditional deletion of *Dicer* in adult mice cause progressive and selective degeneration of DA neurons (Chmielarz et al., 2017). In the same study, another model, termed *Dicer*^{HET}, was also introduced. The model is based on heterozygous *Dicer* deletion, which leaves the animals only one copy of functional *Dicer* allele. The purpose of this was to model age-related Dicer downregulation more accurately. Although, it should be noted here, that reduced Dicer expression levels were never confirmed. In *in vivo* experiments, *Dicer*^{HET} animals at 10 weeks post *Dicer* deletion exhibited decreased levels of striatal DA and its metabolites compared to control animals. In line with the documented gender differences in PD, DA reduction was observed to be more pronounced in the male animals (Moisan et al., 2016). Moreover, even though there was no apparent cell death, older male animals began to develop PD-like locomotor symptoms, indicating an impairment in DA neuron function. Consistent with these findings, it was also demonstrated that boosting Dicer activity, by pharmacological stimulation with enoxacin, protected DA neurons from PD related insults. This aspect was addressed in cultured cells derived from the VTA region of mice, where a constitutive system (*Dat -Cre* instead of *Dat -CreER*^{T2}) was applied to produce the *Dicer*^{HET} genotype. Nevertheless, this case demonstrates that promoting pre-miRNA processing through agents that boost Dicer activity could be a promising mean for neuroprotection. It is also evident that the *Dicer*^{HET} *in vitro* model could serve as a valid tool for investigating neurodegeneration and protection and as such it could be of clinical value. Thus, there remains a need to develop more sophisticated conditional recombination strategies for inducing *Dicer* recombination *in vitro*.

3 Aims of the study

The overall aim of this project was to model Dicer downregulation *in vitro* for studying effects of global miRNA dysregulation in Parkinson's disease. More specifically, our goal was to achieve the earlier proposed *Dicer*^{HET} model in neuronal cultures by using a more practical and convenient knockout method than previously, allowing a more precise temporal control over recombination in a promoter-independent manner. In brief, we combined the *Cre/loxP* recombination system and lentiviral delivery of Cre recombinase. Hence, our specific objectives were;

I. To validate the method by confirming successful knockout of the floxed *Dicer* allele (in *Dicer*$^{flox/+}$ primary mouse cortical cultures).

II. To optimize the transduction protocol for maximal recombination efficiency.

III. To investigate (for the first time) if heterozygous *Dicer* deletion leads to Dicer downregulation at transcriptional and translational levels.

Another important aim of this project was to validate the established model by using it in a relevant experiment. This would allow us to test our hypothesis on the relationship between Dicer downregulation and PD related conditions. Hence, our last objective was;

IV. To conduct a preliminary experiment to study effects of heterozygous *Dicer* deletion on progression of PFF-induced LB-pathology.

4 Materials and Methods

4.1 Human cell culture

We used mycoplasma free HEK293T cells (ATCC, CRL-1573) to produce and propagate the lentiviral vectors desired in the present project. Cells were cultured in sealed 25-cm^2

flasks in Dulbecco's Modified Eagle Medium (DMEM; Cat No. 12491-015, Thermo Fisher Scientific, Inc., Grand Island, NY, USA) supplemented with 10% fetal calf serum (FBS; Cat No. 10500056, Thermo Fisher Scientific, Inc., Grand Island, NY, USA) and 100 μg/ml normocin (Cat No. ant-nr-2, Invivogen, San Diego, CA, USA), unless otherwise stated. The cultures were maintained in an incubator at 37°C under a humidified atmosphere (water saturated) containing 5% CO_2 and were passaged every 3-4 days. Cell passage was performed as follows. Growth media was removed from confluent cultures with a vacuum pump and cells were washed with 5 ml of 1× PBS to remove floating dead cells and any traces of serum that could inactivate proteolytic action of trypsin. Cells were then brought into suspension by detaching them with 1-minute incubation with 1 ml of trypsin-EDTA at 37°C and subsequent addition of 5 ml of growth media. After cells were homogenized by aspiration, they were transferred to a falcon tube and centrifuged for 5 minutes at 300 × g. Cell pellets were then resuspended in fresh growth media and seeded to a new culture at required density. All solutions were prewarmed to 37°C prior to use on cells. Cells were always handled in a sterile environment and proper aseptic techniques were maintained thorough all procedures.

4.2 Lentiviral production and concentration procedures

Cre recombinase expression in neuronal cultures was mediated by VSV.G pseudotyped lentiviral vectors (LvVs). We used an HIV-1 virus based, third-generation system, consisting of two packaging plasmids, an envelope plasmid and a transfer plasmid (Table 1). To produce the infectious viral particles, packaging cells (HEK293T) were first transiently cotransfected with the four-plasmid system using PEI transfection and then subjected to purification and concentration procedures. We implemented a high yield packaging protocol that is described with more details below. All the experiments involving infectious LvVs were performed in a biosafety level 2 facility in accordance with the aseptic requirements.

Table 1 Plasmids encoding lentiviral vector components. Indicated plasmids were used in this work to produce the desired lentiviral particles. Plasmids in the packaging mix were used with either one of the indicated transfer plasmids to produce different vectors.

Packaging mix		
pMDLg/pRRE	Packaging plasmid	Encodes HIV1-GAG/POL
pRSV/REV	Packaging plasmid	Encodes HIV1- REV
pMD2.G	Envelope plasmid	Encodes VSV glycoprotein
Transfer plasmid (either one)		
pCDH-hSYNGFP-T2A-Cre	Transfer vector plasmid	Encodes the insert gene(s)
lenti-hSYN-T2A-GFP (control)		Encodes the insert gene

4.2.1 Isolation of vectors from bacterial stocks

Plasmids pMDLg/pRRE, pRSV/REV and pMD2.G were gifts from Didier Trono (Cat. No. 12251, 12253 and 12259, Addgene, Watertown, MA, USA). pCDH-hSYNGFP-T2A-Cre and lenti-hSYN-T2A-GFP constructs were previously cloned in our lab. Plasmids were propagated and maintained in *E.coli* strains DH5α(pMDLg/pRRE), DH5α(pRSV/REV), DH5α(pMD2.G), DH5α(pCDH-hSYNGFP-T2A-Cre) and DH5α(lenti-hSYN-T2A-GFP) stored in -80°C as glycerol stocks until needed. To extract the plasmids, starter cultures were made from glycerol stocks in 2 ml of Luria-Bertani medium supplemented with 0.1 mg/ml of ampicillin and incubated at 37°C on an orbital shaker at 222 rpm overnight. Each starter culture was reinoculated into 200 ml of Luria-Bertani medium supplemented with 0.1 mg/ml of ampicillin and grown in 2 L shake flasks in the same conditions overnight. Plasmid DNA (pDNA) purification was performed using a commercial kit (NucleoBond® Xtra Midi DNA, Cat. No. 740410.50, Macherey-Nagel, Düren, Germany). Rest of the procedures were carried on following the manual provided by the manufacturer. Plasmids were eluted each in 300 µl of 1× TE buffer and quantified using UV spectrophotometry (OD A_{260} and A_{280}) (Nanodrop™ 2000, Thermo Fisher Scientific, Inc., Wilmington, DE, USA) and stored at -20°C until needed. DNA concentrations were between 0.8-1.2 µg/µl with purity levels (OD A_{260}/ A_{280}) above 1.87.

4.2.2 Preparation of packaging cells

Following describes procedures implemented per lentiviral vector. To start the viral production, cells at passage 8 (P8; for high transfection efficiency under P20 preferable) were taken from the flask stocks and seeded in 4 10-cm petri dishes at 1.1×10^6 cells per dish in 10 ml of growth medium (described under human cell culture). Cultures were grown until 90% confluency (3 days) and were then split with 1:3 ratio into 12 dishes containing growth medium supplemented with 25 mM HEPES (N-2-hydroxyethylpiperazine-N-2-ethane sulfonic acid; Cat No. 15630080, Thermo Fisher Scientific, Inc., Grand Island, NY, USA). Prior to transfection, cells were allowed to adhere for 24 hours until they reached approximately 80% confluency.

4.2.3 PEI stocks

Transfer and packaging plasmids were introduced into the cells by polyethylenimine (PEI) transfection reagent. To prepare a PEI stock solution 50 mg linear PEI (molecular weight, 25 kDA; Cat. No. 23966-2, Polysciences Inc., Warrington, PA, USA) was added to 50 ml 1× PBS (pH adjusted to 4.5 with HCl) and heated in 75°C water bath and vortexed every 10 minutes until the solution was homogenized. Solution was then cooled to room temperature and filtered through a 0.22 μm filter, prior to storage at 4°C.

4.2.4 PEI-mediated transient transfection

In total 12 culture dishes were infected for production of each lentiviral vector. Per dish, DNA mixture was prepared by diluting 4 μg of the transfer plasmid (pCDH-hSYNGFP-T2A-Cre or lenti-hSYN-T2A-GFP) and 2 μg of each helper plasmids (pMDLg/pRRE, pRSV/REV and pMD2.G) into 500 μl of pre-warmed serum-free OptiMEM II medium (Cat. No. 1985070, Thermo Fisher Scientific, Inc., Grand Island, NY, USA). Next, 40 μl of PEI solution (1 μg/μl in 1× PBS pH4.5) was added to the mixture to get 4:1 v/w ratio of PEI:DNA. The resulting PEI:DNA:OptiMEM mixture was vortexed briefly (10 s) and incubated at room temperature for ≥10 min. Transfection mixture, containing 10 μg of total pDNA, was then applied to each culture dish in a dropwise manner and mixed with the culture medium by swirling the dishes briefly. Cultures were incubated for 72 hours at 37°C in a 5% CO_2 humidified atmosphere. During incubation, transfectants were inspected

under a fluorescent microscope for GFP expression to confirm a successful transfection and viral production.

4.2.5 Viral collection and concentration

LvVs were harvested from the growth medium 72 hours post-transfection, by the time over 80% of the cells were observed to express the fluorescent marker. Growth media, containing lentiviral particles, were transferred from plates to 50 ml falcon tubes and centrifuged at room temperature for 5 minutes at 300 × g to remove cellular debris. Supernatant was further filtered through a 0.45 μm pore filter to remove remaining debris. Following this, virus concentration was performed instantaneously. Clarified viral filtrate was transferred to 3 Ultra-Clear centrifuge tubes (38.5 ml tubes; Cat. No. 344058, Beckman Coulter, Inc., Brea, CA, USA) fitted into metal rotor tubes compatible with AH-629 ultracentrifuge rotor (Beckman Coulter, Inc., Brea, CA, USA). Tubes were carefully equalized and centrifugation was performed at 120,000 × g for 1.5 hours, at 4°C. Supernatants were poured out and the tubes were turned upside down on a paper towel to drain for 3 minutes to ensure the complete disposal of the medium (serum damages viral particles). Dried pellets containing viral particles were each re-suspended in 60 μl of sterile Dulbecco's phosphate-buffered saline (DPBS; Cat No. 14287-080, Thermo Fisher Scientific, Inc., Grand Island, NY, USA), combined in one 1.5 ml Eppendorf tube and centrifuged on a benchtop centrifuge for 1 min at 17,000 × g to remove any remaining cellular debris. At last, viral supernatant was collected, aliquoted to and stored at -80°C.

4.3 Heterozygous *Dicer* knockout in primary neuronal cultures

4.3.1 Mouse strains

In our experiments, we used transgenic NMRI mouse embryos with a heterozygous floxed *Dicer* gene allele, referred to as $Dicer^{flox/+}$. All animal experiments were conducted according to 3Rs mandates of the current EU legislation (Directive 2010/63/EU) on the protection of animals used for scientific purposes and Finnish laws and regulations, including Finnish act [497/2013] on the Protection of Animals Used for Scientific or Educational Purposes and government decree [564/2013] on the Protection or Animals Used for Scientific or

Educational Purposes. Protocols were approved by the Finnish National Board of Animal Experiments.

4.3.2 Preparation of cortical primary neuron cultures

Primary neuronal cultures were prepared from mouse embryos at gestational day 16 (E16) or E15. Cultures from each litter was prepared on separate occasions. Pregnant mice were sacrificed by CO_2-anaesthesia and their embryos were removed from the amniotic sacs and placed in ice cold DPBS (Cat No. 14287-080, Thermo Fisher Scientific, Inc., Grand Island, NY, USA) with 0.2% bovine serum albumin (BSA) (Cat. No. A4161, Sigma-Aldrich, St. Louis, MO, USA). Under a stereoscopic microscope, brains were squeezed out from decapitated heads and moved to a separate dish with fresh ice-cold DPBS + 0.2% BSA solution. Cortices were dissected from the brain lobes and cut to several pieces (~3 pieces/cortex). The chopped-up brain segments were collected with a pipet and transferred into a 15-ml falcon tube buried in ice. The tissues were allowed to settle, and the supernatant was pipetted out and replaced with 2 ml of Hank's Balance Salt Solution (HBSS; Cat. No. 14025092, Thermo Fisher Scientific, Inc., Grand Island, NY, USA). Subsequently, 100 µl of 2,5% trypsin (Cat. No. 15090046, Thermo Fisher Scientific, Inc., Grand Island, NY, USA) was added, and the tissues were moved to 37°C water bath to be incubated for 15 minutes. During this time, tissues were mixed by inverting the tube gently every 5 minutes. Simultaneously, 15 ml of HBSS+ 10% FBS (Cat No. 10500056, Thermo Fisher Scientific, Inc., Brazil) solution was prepared and warmed up in the water bath. Following the incubation, 3 ml of prewarmed HBSS+ 10% FBS solution was added to the tissues (total volume 5 ml) to neutralize the trypsin. Further, 50 µl Dnase I (10 mg/ml; Cat. No. 11284932001, Roche Diagnostics, Mannheim, Germany) was added and promptly the tube was inverted 3 times to dissociate the tissues. Next, the tube was centrifuged (Centrifuge 5415D, Eppendorf, Hamburg, Germany) at 500 rpm for 30 seconds, in order to wash the cells. Supernatant was removed carefully and another 5 ml of warm HBSS+ 10% FBS solution was added to the cells. Once again, cells were centrifuged, and the supernatant was removed, in the same manner. Now, cells were resuspended in 2 ml of warm Neurobasal medium (NB; Cat. No. 21103049, Thermo Fisher Scientific, Inc., Grand Island, NY, USA) and they were centrifuged again as previously. The supernatant was collected to a new 15-ml falcon tube and the pellet was discarded. Hereafter, cells were centrifuged for 2 mins at 800 rpm. Supernatant was removed and 2 ml of warm culture

medium (NB-medium supplemented with 2% B27 (Cat. No. 17504044, Thermo Fisher Scientific, Inc., Grand Island, NY, USA) and 0.5 mM L-Glutamine (Cat. No. A2916801, Thermo Fisher Scientific, Inc., Grand Island, NY, USA) was added to the pellet. Finally, to dissociate the cells, pellet was aspirated well by gently passing the cells 20-40 times through a pipette.

Viability of the resuspended neurons were assessed with TC20™ automated cell counter (Bio- Rad laboratories, Inc., Hercules, CA, USA) that is based on the standard trypan blue staining. Sample solution was prepared by mixing 20 µl of cell suspension and 20 µl of 0.4 % trypan blue solution (Cat. No. 15250061, Thermo Fisher Scientific, Inc., Grand Island, NY, USA). Based on this, cells were diluted with warm culture medium to appropriate concentrations and seeded on 0,5 mg/ml poly-DL-ornithine coated plates (in 0.15 M Boric acid, pH 8.7) that were prepared on the previous of day. For western blot assays cells were plated on 6 well plates and for qPCR, genotyping and microscopy studies cells were plated on 96-well plates. For microscopy studies we used clear bottomed 96-well ViewPlate microplates (Cat. No. 6005182, PerkinElmer, Inc., Turku, Finland). 96-well plates were seeded at 50,000 cells/well in 100 µl of the cell dilution, and the 6-well plates were seeded at 500,000 cells/well in 2 ml of the cell dilution. To prevent loss of medium by evaporation, outer wells of the 96-well plates were filled with sterile H_2O. Cultures were allowed to grow in an incubator at 37°C and 5% CO_2 and fed by changing half of the culture medium at 3 days in vitro (DIV) and thereafter approximately once a week until transductions were completed, and cells were harvested. Detailed schedules of the experiments can be seen on Figure 3.

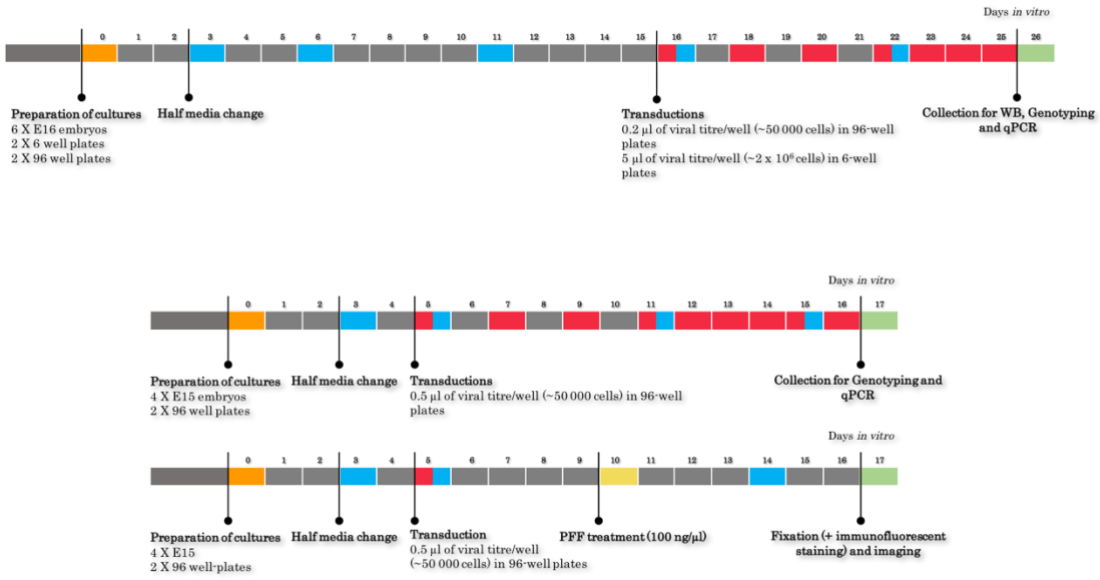

Figure 3 Schematic timeline of the knockout experiments.

4.3.3 Lentiviral transduction

To establish the method, cultures were first transduced on various time points, and with different viral titres. Transduction time points in these and the following experiments are presented in Figure 3. To transduce cultures on 96-well plates (50 000 cells/well), appropriate volume of the concentrated lentiviral vector was diluted in NB-medium and 10 µl of this dilution was added to each well. Final volume of the viral concentrate was either 0.2 µl/well or 0.5 µl/well (Figure 3). To infect the cultures on 6-well plates, 5 µl of the viral concentrate was used per each well (2×10^6 cells/well). Similarly, transductions were carried out by diluting appropriate volume of the viral concentrate in NB-medium, and 100 µl of the dilution was used to infect the cells.

4.3.4 PFF treatment

Recombinant mouse αSyn pre-formed fibrils (PFFs; 5 mg/ml; stocked and stored at -80°C) were thawed for 10 min at room temperature, diluted in 1× PBS (1:50) and sonicated at high power (10 cycles, 30 seconds on/ 30 seconds off) using Bioruptor® sonicator (Diagenode, Liege, Belgium). PFFs were further diluted in NB-medium and applied to the cultures by replacing 75 µl of the culture medium with the PFF dilution, giving a final

concentration of 2.5 μg/mL. On the control wells, an equivalent volume of medium was replaced with fresh NB-medium. All PFF treatments were performed 5 days post-transduction (DIV10). Sonications and dilutions were made immediately before use.

4.4 Genotyping

4.4.1 DNA extraction

DNA was extracted from the neocortical cell cultures using a commercially available product, AccuStart II PCR genotyping kit (Cat. No. 95135-500, QIAGEN Beverly, Inc., Beverly, MA, USA). DNA extraction was carried out according to the manufacturer's manual. Briefly, all media was removed from the wells and cells were washed once with 50 μl of cold 1× PBS. 50 μl of extraction buffer was added to each well and aspirated 5 times to disattach the cells. Samples were transferred each to 1.5 ml tubes and incubated at 95°C for 30 minutes. Hereafter, DNA lysates were cooled for 10 minutes in room temperature and placed in ice until further procedures. 1.2 μl of the lysates were used in a PCR reaction or alternatively mixed with 50 μl of stabilization buffer and kept at -20°C, until further processed.

4.4.2 PCR amplification

The extracted DNA samples were amplified in a multiplexed PCR that was designed to detect the presence of wild type, floxed and deleted *Dicer* allele. We used three *Dicer* specific primers (Metabion international AG, Planegg, Germany), two forward and one reverse, all with the annealing temperature of 58°C. Primer sequences and their expected product sizes are presented in the Table 2. The final reaction volume for each sample was 12 μl, consisting of 1.2 μl of DNA lysate, 6 μl of 2× reaction buffer (AccuStart II GelTrack PCR SuperMix, Cat. No. 95136-500, Quanta Biosciences, Beverly, MA, USA), 0.5 μl of each of the primers and 3.3 μl of double distilled water (ddH_2O). The PCR reactions were run in a Thermal Cycler (SimpliAmp^{TM} Thermal Cycler, Life technologies, Singapore) using the program indicated in Table 3.

Table 2 Primers used to genotype the cultures. Combination of 3 PCR primers amplify specific products for each possible *Dicer* allele present in the cultures. Sequences 5'-3'. R indicates reverse and F indicates forward.

	Primer sequence	Amplicon size (bp)
32050 AS	R: CTGGTGGCTTGAGGACAAGAC	259 (wildtype) or 390 (floxed)
31831	F: AGTGTAGCCTTAGCCATTTGC	
28290	F: AGTAATGTGAGCAATAGTCCCAG	309 (deleted)
32050 AS	R: CTGGTGGCTTGAGGACAAGAC	

bp = base pair, R = reverse, F = forward

Table 3 PCR program used to genotype the cultures.

	Phase	Temperature (℃)	Time
	Denaturation	95	3 min
Cycle × 30 times	Denaturation	95	30 s
	Annealing	55	30 s
	Extension	72	30s
	Final extension	72	10 min
	Final hold	16/4	For ever

4.4.3 Agarose gel electrophoresis (AGE)

PCR products were analysed by visualizing them on agarose gel electrophoresis (AGE). 2.5% agarose gel was prepared in 1× tris acetate-EDTA (TAE) buffer and 1:10000 ethidium bromide (EtBr; 0.626 mg/ml; Cat. No. C997H52EA, Amresco, Inc., Solon, OH, USA). GeneRuler 50 bp DNA Ladder (Cat. No. SM0373, Thermo Fisher Scientific, Inc., Waltham, MA, USA) was used as a molecular standard. Gels were run at 120 mV in 1× TAE buffer until the dye markers reached 2/3 of the gel (~40 min). DNA was visualized and documented with a UV camera (ChemiDoc MP imaging system, Bio-Rad laboratories, Inc., Mississauga, ON, USA).

4.5 Western blot

4.5.1 Lysis of cortical neurons

To release the proteins cells were harvested, washed and lysed. To do this, media was carefully removed and replaced with 2 ml of 1× PBS (per well) to wash the cells. PBS was discarded and 100 µl of lysis buffer (1% NP-40, 0.15 M NaCl, 50 mM Tris pH 7.4, 1 mM EDTA) was added to each well. Bottom of the wells were scraped with a rubber cell scrapper and cell scrapings were transferred to 1.5 ml Eppendorf tubes. Protein concentrations were determined, using UV spectrophotometry (Nanodrop 2000, Thermo Fisher Scientific, Inc., Wilmington, DE, USA), and the samples were stored at -20°C until SDS-PAGE was performed.

4.5.2 sodium dodecyl sulphate-polyacrylamide gel electrophoresis (SDS-PAGE)

Proteins were separated on 4-12% gradient polyacrylamide precasted gels (NuPAGE™ Bis-Tris mini gels, Cat. No. NP0322BOX, Thermo Fisher Scientific, Inc., Waltham, MA, USA) under denaturing conditions. Two gel cassettes were prepared as directed in the instructions provided by the manufacturer and the cassettes were assembled in the electrophoresis apparatus. Chambers were filled with 1× NuPAGE™ MOPS SDS Running Buffer (Cat. No. NP000102, Thermo Fisher Scientific, Inc., Waltham, MA, USA) and 5 µl of pre-stained molecular weight marker, Precision Plus Protein™ Dual Color Standards (Cat. No. 161-0374, Bio-Rad laboratories, Inc., Mississauga, ON, USA) was loaded to the first wells of each gels. Protein samples were denatured by mixing 8 µl of thawed cell lysate with 2 µl of Laemmli sample buffer (65.8 mM Tris-HCl (pH 6.8), 26.3% (w/v) glycerol, 2.1% SDS, 0.01% bromophenol blue and 5% B-mercaptoethanol) and incubated 5 mins at 90°C (HB-2 block heater, Wealtec Corp., Sparks, NV, USA). Samples were then centrifuged (13,000 rmp; 1 min), loaded onto the gels and subjected to electrophoresis by applying 200 V constant voltage for 40 minutes (Mini protean® Electrophoresis System, Bio-Rad laboratories, Inc., Mississauga, ON, USA).

4.5.3 Membrane transfer and immunodetection

Once the proteins were separated by SDS-PAGE, they were transferred onto a nitrocellulose membrane using a wet western transfer method. All the steps in the procedure were undertaken at room temperature and all incubation and washing steps during the staining procedure were performed on an orbital shaker, unless otherwise mentioned. Briefly, the gels were washed with water and equilibrated in 1× transfer buffer (20% v/v methanol, 0.19M glycine and 0.05M Tris) for 15 minutes. Transfer cassette equipment, including nitrocellulose membrane (Thermo Fisher Scientific, Inc., Waltham, MA, USA), filter papers and pads, were pre-immersed in 1× transfer buffer as well and subsequently arranged into a "sandwich" with the gel and the membrane in the middle. The transfer cassettes were placed into transfer tanks and the tanks were filled with ice cold transfer buffer. Blotting was performed at 100 V constant voltage for 60 minutes (Mini Trans-Blot® system, Bio-Rad laboratories, Inc., Mississauga, ON, USA).

After a successful transfer, membranes were blocked overnight with 5% skimmed dried milk (blocking buffer) in TBST (Tris-buffered saline + 0.1% Tween). Next, membranes were placed in primary antibody solution (Table 4) and incubated overnight at + 4°C. On the following day, membranes were rinsed with TBST-solution, and washed 3 times by immersing them in TBST for 10 minutes each time. Membranes were then incubated in blocking buffer for 1 hour, and subsequently placed in secondary antibody solution (Table 4) to be incubated for 1 hour. Finally, membranes were rinsed and washed once in TBST and washed twice in 1× TBS (10 min/wash). To visualize the protein bands, membranes were scanned using Odyssey®CLx Infrared Imaging System (LI-COR, Inc., Lincoln, NE, USA).

Table 4 Antibodies used in Western Blot (WB). Primary mouse monoclonal antibody against Dicer and primary rabbit monoclonal antibody against β-actin and infrared dye-conjugated secondary goat anti-Rabbit IgG and goat anti-Mouse IgG were used in WB experiments. Primary antibodies were diluted in blocking buffer (5% skimmed dried milk in TBST (Tris-buffered saline + 0.1% Tween)) before being applied to nitrocellulose membranes. Similarly, secondary antibodies were diluted in blocking buffer (5% skimmed dried milk in TBST (Tris-buffered saline + 0.1% Tween)). Antibodies, their antigens, species, dilutions and sources are indicated.

Antibody	Antigen	Species	Dilution	Source
Dicer	Dicer	Mouse	1:1000	Cat. No. ab14601, Abcam, Cambridge, MA, USA
β-actin	β-actin	Rabbit	1:2000	Cat. No. 926-42210, LI-COR, Inc., Lincoln, NE, USA
IRDye® 680LT	Mouse IgG	Goat	1:10000	Lot. No. C60301-03, LI-COR, Inc., Lincoln, NE, USA
IRDye® 800CW	Rabbit IgG	Goat	1:10000	Lot. No. C60321-05, LI-COR, Inc., Lincoln, NE, USA

4.6 Quantitative reverse transcription PCR (RT-qPCR)

In order to assess the expression levels of *Dicer* mRNA, a quantitative reverse transcription PCR (RT-qPCR) was performed, using reagents provided by TaqMan® Gene Expression Cells-to-C_T™ Kit (Cat. No. AM1729, Life Technologies, Carlsbad, CA, USA) and TaqMan® Gene Expression assays (Life Technologies, Carlsbad, CA, USA). The kit was used according to protocols that were largely based on manufacturer's instructions, as described below.

4.6.1 RNA extraction

Total RNA was extracted by lysing the cells and eliminating genomic DNA. To do this, growth media was discarded from the cultures and cells were washed once with 50 µl of cold 1× PBS. 50 µl of lysis solution, containing 1:100 Dnase I, was added to each well, triturated carefully 5 times and allowed to incubate for 5 minutes at room temperature. Next, 5 µl of stop solution was added to the cell lysates, mixed carefully and thoroughly by triturating 5 times and allowed to incubate for 2 minutes to completely inactivate the lysis reagent. Lysates were stored at -20°C until needed for cDNA synthesis.

4.6.2 Reverse transcription (RT)

RNA, released into cell lysates, were reverse transcribed into their DNA complements (cDNA) by performing a reverse transcription polymerase chain reaction (RT-PCR). RT-reactions were run in 50 µl reaction volumes, containing 10 µl cell lysate 25 µl 2× RT buffer, 2.5 µl 20× RT Enzyme Mix and 12.5 µl nuclease free water. Further, two different negative controls were included to confirm that the template is cDNA and not gDNA (minus-RT negative control) and to avoid results from possible DNA contamination (no-template control). Minus-RT negative control was prepared without the 20× RT enzyme mix and the no-template control was prepared without the cell lysate (volumes of the excluded components replaced with H_2O). Reactions were incubated in a PCR machine (SimpliAmp™ Thermal Cycler, Life technologies, Singapore) using the following conditions: reverse transcription at 37°C for 60 minutes and inactivation at 95°C for 5 minutes. The cDNA products were kept at -20°C until qPCR was performed.

4.6.3 Quantitative PCR (qPCR)

The obtained RT products were amplified in quantitative PCR (qPCR) using LightCycler® 480 system (Roche, Indianapolis, IN, USA). Reactions were run on LightCycler® 480 Multiwell Plates 384 (Roche, Indianapolis, IN, USA) each in 10 µl volume, consisting of 5 µl of 2× TaqMan® Gene Expression Master Mix, 0.5 µl of 20× TaqMan® Gene Expression Primers, 2.5 µl of nuclease-free water and 2 µl of cDNA. Housekeeping gene GAPDH was used as a reference gene to normalize the mRNA levels of the target gene (*Dicer*). Following primer pairs were used: for *Dicer* 5'-GTACGACTACCACAAGTACTTC-3' and 5'-ATAGTACACCTGCCAGACTGT-3' and for GAPDH 5'-CCACCCATGGCCAAATTCCATGGCA-3' and 5'-TCTAGACGGCAGGTCAGGTCCACC-3'. All reactions, including the controls, were carried out in duplicates and each well was subjected to three repeated measurements. qPCR conditions were as described in Table 5.

Table 5 qPCR program used for gene expression analysis of *Dicer*.

	Phase	Temperature (℃)	Time
	UDG incubation	50	2 min
	Enzyme activation	95	10 min
Cycle × 40 times	Denaturation	95	15 s
	Amplification	60	1 min

UDG = Uracil-DNA glycosylase

4.7 Immunofluorescent staining

Neuronal nuclei (NeuN) and phosphorylated (at Ser129) αSyn (pSer129-αSyn) were visualized in PFF-treated cultures by immunofluorescence staining. All steps in the staining procedure were undertaken at room temperature unless otherwise mentioned. Cultured cells were fixed for staining in 4% paraformaldehyde in 1× PBS for 20 minutes, followed by 2 sequential washes with 1× PBS, 15 mins treatment with permeabilization solution containing 0.2% Triton X-100 made in 1× PBS (0.2% PBST) and 1 h blocking with 0.2% PBST containing 5% (w/v) normal horse serum (blocking buffer; Cat. No. s-2000, Vector Laboratories, Inc., Burlingame, CA, USA). Cells were incubated overnight at + 4°C with primary antibodies diluted in blocking buffer (Table 6). Next day, staining was resumed by washing the cells three times with blocking buffer and treating them for 1 hour with secondary antibodies diluted in 0.2% PBST (Table 6). Wells were further washed three times with 1× PBS and incubated for 10 mins in a 0.2 mg/ml 4',6-diamidino-2-phenylindole (DAPI; Cat. no. D1306, Thermo Fisher Scientific, Inc., Waltham, MA, USA) solution, followed by two final washes with 1× PBS. Finally, 100 µl 1× PBS was added to each well and plates were stored at + 4°C until imaging.

Table 6 Antibodies used in immunofluorescence staining to visualize neuronal nuclei (NeuN) and phosphorylated (at Ser129) αSyn (pSer129-αSyn). Primary mouse monoclonal antibody against NeuN, primary rabbit monoclonal antibody against pSer129-αSyn and AlexaFluor 568- or Alexa Fluor 647–conjugated secondary antibodies against mouse or rabbit IgG were used in immunofluorescence staining of the PFF-treated cultures. Primary antibodies were diluted in blocking buffer (5% (w/v) normal horse serum in 0.2% PBST (0.2% Triton X-100 made in 1× PBS)) before being applied to the cultures.

Similarly, secondary antibodies were diluted in 0.2% PBST (0.2% Triton X-100 made in 1× PBS). Antibodies, their antigens, species, dilutions and sources are indicated.

Antibody	Antigen	Species	Dilution	Source
Anti-NeuN	NeuN	Mouse	1:500	Cat. No. MAB377, Millipore, Billerica, MA, USA
Anti-Alpha-synuclein	pSer129-αSyn	Rabbit	1:2000	Cat. No. ab51253, Abcam, Cambridge, MA, USA
AlexaFluor 568	Mouse IgG	Donkey	1:500	Cat. No. A10037, Thermo Fisher Scientific, Inc. Waltham, MA, USA
AlexaFluor 647	Rabbit IgG	Donkey	1:500	Cat. No. A31573, Thermo Fisher Scientific, Inc. Waltham, MA, USA

NeuN = Neuronal nuclei, pSer129-αSyn = phosphorylated αSyn at residue Ser129.

4.8 Automated high throughput microscopy and data analysis

4.8.1 Automated high throughput microscopy

Immunofluorescence was captured with an epifluorescent microscope, Cellinsight CX5 High Content screening (HCS) platform (Thermo Fisher Scientific, Inc., Waltham, MA, USA) equipped with a Quantix CCD camera (Photometrics, München, Germany) running at 1024 × 1024 resolution and 2 × 2 binning (resulting in 512 × 512 images). Images were acquired using Thermo Scientific™ HCS Studio™ software and a 10X objective 0.45NA (Olympus Plan Apo 10×/0.45, Nikon, Japan) at a resolution of 1.17 μm/pixel. Per well, images of 16 view fields were acquired in 4 × 4 grid patterns and at different wavelengths, producing 4 replicates for each field of view. DAPI stained nuclei ($\lambda_{ex/em}$ = 358/461 nm) were detected using excitation filter at 386/23 nm and 3.43 ms exposure time, GFP fluorescence ($\lambda_{ex/em}$ = 395/509 nm) was detected in a second channel at 485/20 nm and 50 ms exposure, NeuN fluorescence ($\lambda_{ex/em}$ = 578/603 nm) in a third channel at 549/15 nm and 200 ms exposure and pSer129-αSyn fluorescence ($\lambda_{ex/em}$ = 650/665 nm) in a fourth channel at 650/13 nm and 150 ms exposure.

4.8.2 Image processing and segmentation

Captured images were automatically identified and quantified by using open source softwares, CellProfiler and CellProfiler analyst 2.0 (Carpenter et al., 2006; Jones et al., 2008;

Jones et al., 2009). Two customized and coupled pipelines were used to assess the survival of the neurons and to subsequently analyse the LB-like aggregates in the survived neurons based on multiple measured properties and features. Nuclei and the cell borders were identified utilizing the DAPI and NeuN channels and the LB-like aggregates based on pSer129-αSyn-positive staining in a separate channel. Cell segmentation was performed using Otsu Global thresholding method with threshold correction factor of 1.0. The dataset was classified by utilizing the machine learning algorithms in CellProfiler Analyst software that is able to access the database containing all calculated quantifications. The rules in the algorithms were generated by manual categorization of a number of randomly selected cells into qualitatively negative or positive representatives. Qualification was carried out using merged images and on occasion verified using single channels. In our analysis, mainly gentle boosting was selected to generate the rules, but on some occasions also joint boosting was used. Positive representatives of neurons with LB-like pathology (NeuN cells containing LB-like aggregates) were selected as the few examples presented in Figure 4.

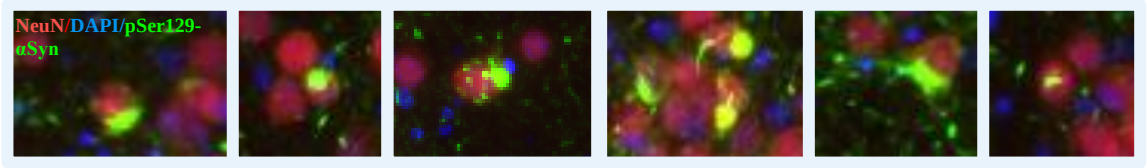

Figure 4 Qualification of cells with LB-like formations. Number of neurons exhibiting pSer129-αSyn pathology were counted by building an automated machine learning model. NeuN-positive cells (red) colocalized with pSer129-αSyn-positive aggregates (green) were fed into the training set as positive representatives. The morphologies passing the qualification were as in the selected images. Moreover, the model was also used to classify different morphologies of pSer129-αSyn-positive aggregates (LB-like or LN-like aggregates). NeuN = Neuronal nuclei, DAPI = 4',6-diamidino-2-phenylindole, pSer129-αSyn = phosphorylated αSyn at residue Ser129.

4.8.3 Data analysis

Data analysis was conducted using GraphPad Prism software 7 (GraphPad Software, Inc., La Jolla, CA, USA). All data comparisons consisted of >2 groups and was analysed by

ordinary one-way analysis of variance (ANOVA) followed by multiple comparison correction using uncorrected Fisher's least significant difference (LSD) for independent pairwise comparison of particular experimental groups. All the graphs in the figures are expressed as mean ± standard deviation (SD) and represent results of four replicates. Differences in means were considered statistically significant at $p < 0.05$. Statistical details are indicated in the captions related to graph figures.

5 Results

5.1 Generation of *DICER^{HET}* mouse primary cortical cultures

We attempted to generate *Dicer^{HET} in vitro* models using Cre expressing lentiviral vectors to delete the *Dicer* allele flanked by *loxP* recognition sequences (floxed) in *Dicer$^{flox/+}$* mouse primary cortical cultures. To our knowledge this is the first report of *Dicer^{HET} in vitro* model generated with this strategy. Hence, we first sought to empirically establish the following parameters for the method; amount of the virus to be used, timing of transduction and required timeframe between transduction and efficient deletion of the floxed *Dicer* allele at genetic, transcriptional and translational levels. To establish these parameters, two experiments were conducted on *Dicer $^{flox/+}$* primary cortical cultures with different experimental setups and analysed by employing PCR based genotyping, Real-Time PCR (qPCR) and western blot techniques. Cultures used for genotyping and qPCR were treated with either 0.2 µl or 0.5 µl of lentivirus concentrate per well containing 5×10^4 cells in 100 µl culture medium. Cultures used for the western blot analysis were infected with 5 µl of lentivirus concentrate per well containing 2×10^6 cells in 2 ml culture medium. Cultures were transduced at different stages, and different age of derivation. The experiments were performed with cultures derived from either mouse embryonic day 16 (E16) or E15 cortical tissue, respectively. Infection of the co-cultures were started either 16 (first experiment) or 5 days (second experiment) after plating and repeated on various time points to appropriate wells during the following days. Expression of the reporter protein GFP was observed under fluorescence microscope in all infected samples 2-3 days following each infection (data not shown), confirming both a successful transduction and subsequent expression of transgenes. The proportion of GFP-positive cells increased with

time and after 5 days about 90% of the cells were observed to be GFP-positive. Cultures were collected for analysis either on DIV26 (first experiment) or DIV17 (second experiment) after 10 or 12 days from the first transduction, respectively. Experimental timelines are illustrated in Figure 5.

A Transduction timeline of the first experiment

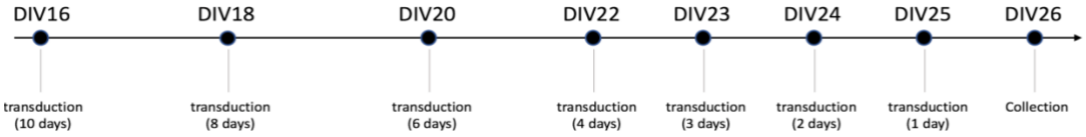

B Transduction timeline of the second experiment

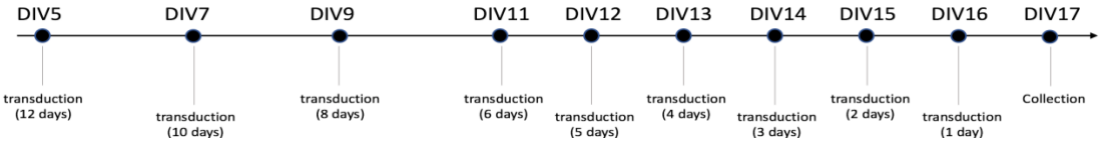

Figure 5 Schematic representation of experimental timelines. Two different experiments were conducted with different settings to establish optimal parameters for generating *Dicer*^{HET} mouse primary cortical cultures employing lenti-hSYN-T2A-Cre virus. Wells in the co-cultures were transduced at different time points in order to determine the time needed from viral infection to achieve efficient recombination. A) Timeline depicting the transduction time points of the first experiment, in which cultures were derived from E16 embryos, transductions performed between DIV16 - DIV25 with 0.2 µl of lentiviral preparation and collected for analysis at DIV26. B) Timeline depicting the transduction time points of the second experiment, in which cultures were derived from E15 embryos, transductions performed between DIV5 - DIV15 with 0.5 µl of lentiviral preparation and collected for analysis at DIV17. For more detailed timelines see materials and methods.

5.1.1 Gene editing efficiency

In order to confirm Cre mediated deletion of the *loxP*-flanked *Dicer* allele in primary cortical cultures and to assess the kinetics of the recombination at a genomic level, cultures were genotyped. To do this we employed a PCR protocol based on a three-primer assay, retrieved from earlier reported *Dicer* deletion experiments (Suárez et al., 2008). The schematic below illustrates the principle of the assay (Figure 6). Briefly, we multiplexed

three primers that span the *Dicer* locus (listed in Table 2) and generate a specific PCR fragment in the presence of each possible *Dicer* allele. As shown in the illustration in Figure 6, primer combination 31831/32050 AS allow to detect the unrecombined alleles by producing a 259 bp fragment in the presence of wildtype allele and a 390 bp fragment in the presence of the floxed allele. The primer combination 28290/32050 AS amplify a 309 bp long product, given that the *loxp* flanked sequence is excised. By this strategy it was possible to determine whether the recombination had taken place based on the presence or absence of predicted PCR products.

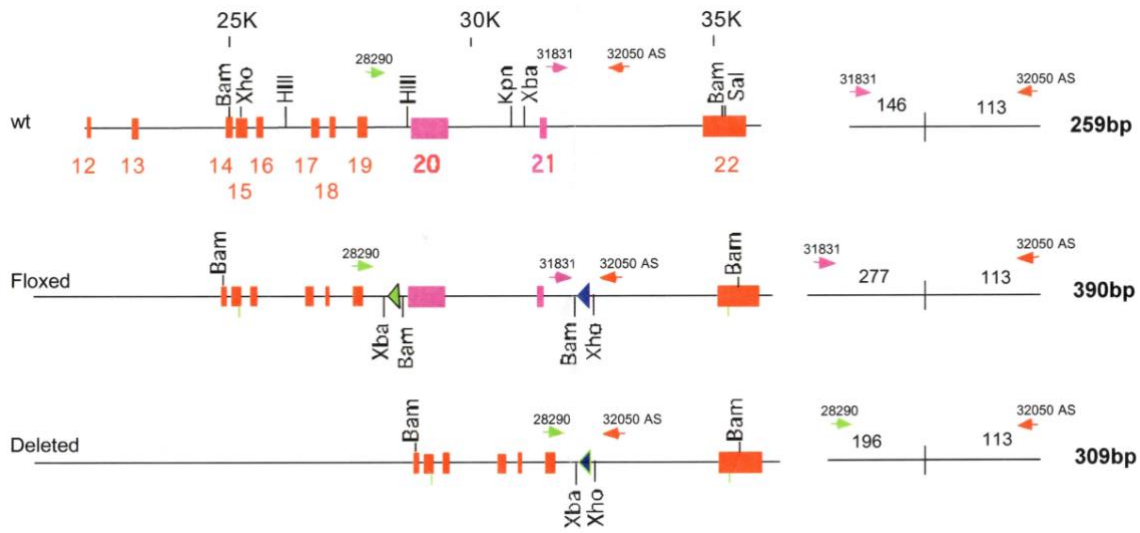

Figure 6 Experimental strategy to analyse recombination of *Dicer* allele. In the left, schematic representation of the *Dicer* alleles with primer localization and in the right, the expected PCR products. Red and purple boxes on the alleles represent exons and blue and green triangles represent *loxP* sites. Position and direction of the primers are denoted with green, purple and red arrows above the diagrams. As shown, primer set 31831/32050 AS amplify unrecombined *Dicer* alleles, producing a 259 bp amplicon from the wildtype (wt) allele and a 390 bp amplicon from the floxed allele. In the presence of the ablated *Dicer* allele, by virtue of recombination that deletes exons 20 and 21, 28290/32050 AS primer pair amplify a 309 bp fragment. 28290 and 32050 AS primers can theoretically also amplify large fragments from the unrecombined alleles, but under the applied PCR conditions amplification of these fragments are inhibited. Illustration adapted from Suárez et al. (2008).

To visualize the results, PCR products were subjected to agarose gel electrophoresis. From the obtained agarose gel images presented in Figure 7, we can see that all amplicon band

patterns were consistent with the predicted PCR product sizes (Figure 6). A lane with two equal bands, in line with 400 and 250 bp ladder bands, represents unrecombined genotype consisting of a floxed and a wildtype *Dicer* allele, and a lane with two equal bands, in line with 250 and 300 bp ladder bands, represents the desired $Dicer^{HET}$ genotype. Samples that have produced bands of all three predicted PCR fragments consist of cells with both genotypes. As can be seen from the results of both experiments (Figure 7A and B), the ~300 bp band indicative of recombined *Dicer* allele ($Dicer^{-}$) is not present in the control cultures (Untreated). These cells were not infected with the lenti-hSYN-T2A-Cre virus. In case of the infected cells, the knockout band ($Dicer^{-}$) becomes detectable at day 2 or 3 postinfection. From these time points onward recombination is evidently ongoing in both experiments, as the ~400 bp band corresponding to floxed *Dicer* allele ($Dicer^{flox}$) gradually fades and the ~300 bp band corresponding to $Dicer^{-}$ intensifies. From these results, we concluded that the transduction and subsequent deletion of the floxed region was successful in both experiments.

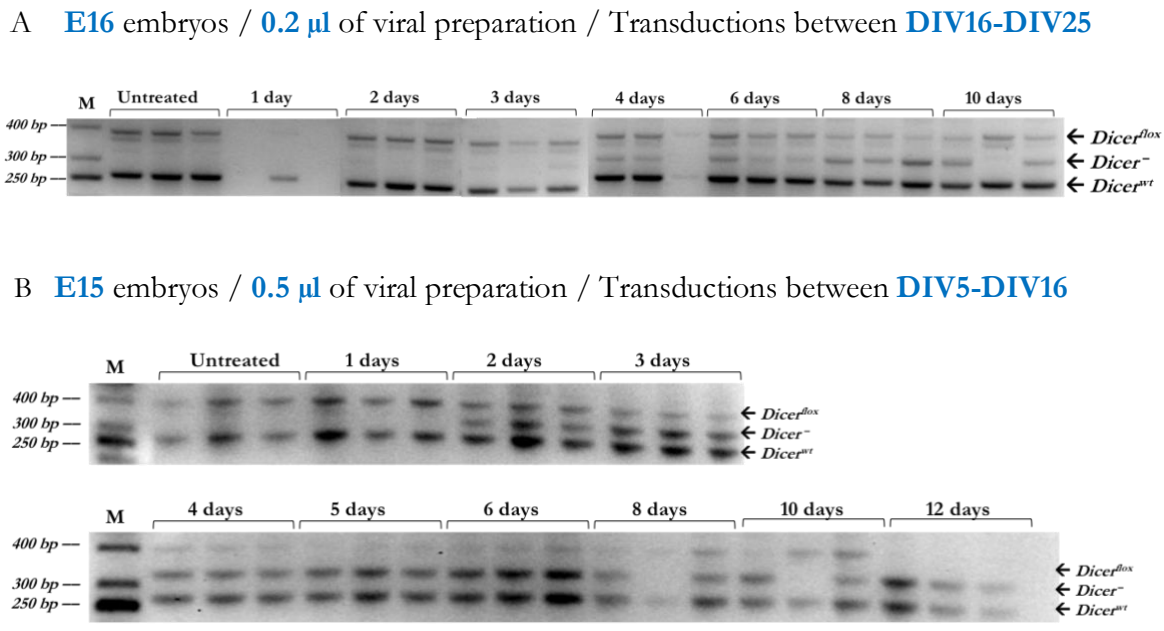

Figure 7 Genotyping of primary cortical cultures to assess kinetics of recombination. Primary cortical cultures, induced at indicated times after infection with lenti-hSYN-T2A-Cre, were genotyped using a three primer PCR assay to verify genetic recombination of floxed *Dicer* allele. Amplicon bands on the agarose gel (2.5%) show that PCR assay has produced fragments that correspond to the expected sizes - 259, 309 and 390 bp. A two-band pattern, located at 400 bp and 250 zones, correspond to an

unrecombined genotype, whilst a two band pattern, located at 400 bp and 300 zones, correspond to the desired *Dicer*^{HET} genotype, consisting of one wild type and one ablated *Dicer* allele. Samples that have produced three bands on their lane, have harbored cells from both recombined and unrecombined genotypes. Results of the first experiment (A) show that recombination has occurred. First sign of recombination appears at day 3 postinfection, manifested by presence of a faint *Dicer*$^{-}$ band, which becomes more visible at later time points. Recombination efficiency however remains low in this case, as the *Dicer*$^{-}$ band fails to reach equal intensity with the *Dicer*^{wt} band and the *Dicer*^{flox} band stays in the background thorough the experiment. Second experiment (B) conducted by changing few variables, produced more conclusive results. Here *Dicer*$^{-}$ bands are more prominent and *Dicer*^{flox} band disappears at day 5 postinfection.

Our first experiment reveals that cortical cultures can be successfully maintained and transduced as late as DIV23. This is in particular an important outcome, as neurons in older cultures resemble mature neurons more than those in younger stages and provide better means for experimentation. However, comparing the results of the two experiments, it can be seen that genetic recombination has occurred at a lower efficiency in the first experiment. As Figure 7A reveals, after the first sign of recombination (DIV3) the *Dicer*$^{-}$ band remains weak in intensity and the *Dicer*^{flox} band does not disappear completely at any indicated time point, resulting in persistent formation of three bands of varying intensities. This indicates that in most cases we acquired cultures with more or less evenly distributed proportions of different genotypes in respect of the *Dicer* gene, rendering the cultures useless for most of our experimental purposes. There could be a number of reasons explaining different yields of genetic recombination between the two experiments. Generally, maturity of neurons and viral titre are the main factors considered in transduction efficiency. In our first experiment, cells were derived from older embryos (E16), treated at more mature stages (DIV16-DIV25) and infected with lower volume of LvV preparation (0.2 µl / 50 000 cells in a 100 µl culture). The result was an incomplete excision of the floxed *Dicer* allele.

To address the recombination efficiency, the abovementioned variables were adjusted in the second experiment. Cultures derived from E15 embryos were transduced between DIV5-DIV16 with 0.2 µl of LvV preparation / 50 000 cells in a 100 µl culture medium. In addition, two more transduction time points, considered appropriate to specify the time needed to achieve maximum recombination efficiency, were introduced. As Figure 7B

shows, *Dicer*⁻ band becomes first detectable at day 2 postinfection, indicating that onset of recombination takes place by this time point. The resulting *Dicer* ⁻ band is explicitly prominent since its first appearance and intensifies as the incubation time increases. Accordingly, the $Dicer^{flox}$ band is smaller and becomes undetectable by day 5 postinfection. It is also worth noting that absence of $Dicer^{flox}$ band correlates with presence of the *Dicer*⁻ band in each lane, furnishing evidence that the employed strategy works as designed. In conclusion, it is evident that with the conditions used in the second experiment, it is feasible to achieve optimum recombination efficiency for deleting the floxed *Dicer* allele in mouse primary cortical cultures. The shortest induction time between transduction and maximum recombination is 5 days, which is short enough to allow experimentation on cultures that on default provide limited time due to their relatively short lifespan. Moreover, pattern of the bands indicates that recombination efficiency is independent on the age of neurons. This argues that the results of the first experiment were weaker because of lower volume of LvVs. For this reason, further validation is recommended to establish the method for older cultures. For now, we concluded any further experiments to be carried out with 0.5 μl of LvV preparation, transductions to be performed between DIV5-12 and all assays to be conducted earliest at day 5 postinfection.

5.1.2 Investigation of transcript and protein levels

Having established the knockout method for producing the $Dicer^{HET}$ cultures, we went on to further characterize the model. The next aims were to investigate whether heterozygous knockout of *Dicer* translates to reduction of *Dicer* transcript and protein levels. These analyses were conducted by performing RT-qPCR and western blot (WB) assay using cell extracts from various time points. Sadly, technical challenges were encountered – the final result of the RT-qPCR could not be retrieved for analysis and the WB image was lost. However, the WB assay proved to be unsuccessful. The analysis revealed no detectable Dicer protein whereas the loading control (β-actin) displayed a clear signal with a correct molecular size. This observation could be attributed to manual processing problems, low levels of Dicer in the samples or potentially quality of the primary Dicer antibody. It should be mentioned that multiple earlier attempts in our lab to detect Dicer with the same antibody have also failed to yield staining. Hence, we suspect that the antibody used lacked reactivity for the claimed target. As this antibody has been specifically raised against human Dicer it is likely that it does not cross-react with mouse Dicer. Unfortunately, the analysis was not repeated as we had not reserved enough time to perform a troubleshooting

investigation and commercialized and appropriately validated antibody against mouse Dicer was not available at the time of the experiments. Therefore, the *Dicer*^{HET} model remains to be further characterized and the abundance of Dicer protein investigated.

5.2 Effects of heterozygous *Dicer* ablation on pathologic αSyn propagation

In an attempt to examine our newly established *Dicer*^{HET} *in vitro* system, we conducted an experiment to assess the effects of Lewy pathology on the cultures. In order to do this, we adopted an extensively used model in which α-synuclein (αSyn) aggregation is seeded by exogenous supply of αSyn pre-formed fibrils (PFFs) (Volpicelli-Daley et al., 2011; Luk et al., 2012). In this model, PFFs mimic the proposed prion-like mechanism of pathogenic form of αSyn. They trigger conversion of endogenous αSyn into insoluble hyperphosphorylated and ubiquitinated proteins that get recruited into aggregates. Our experiments were conducted with mouse primary cortical cultures that were processed according to earlier established parameters. Cultures were derived from E15 *Dicer* $^{flox/+}$ mouse embryos and transduced with either lenti-hSYN-T2A-GFP or lenti-hSYN-GFP-T2A-Cre at 0.5 µl of viral titre on DIV5. As previously, strong GFP signal was detected in >70% of the cells 2 days post-transduction (data not shown), confirming both a successful transduction and subsequent expression of transgenes. Under these conditions, cultures transduced with the lenti-hSYN-GFP-T2A-Cre were expected to bare *Dicer*^{HET} genotype by 5 days post-transduction. Hence, the PFF treatments (2.5 ng/µl) were performed on DIV10. The PFFs that were used had been recently validated in our lab to cause pathogenic aggregation. On DIV18 cultures were fixed and stained for analysis. The experiment was performed according to the experimental timeline in Figure 8.

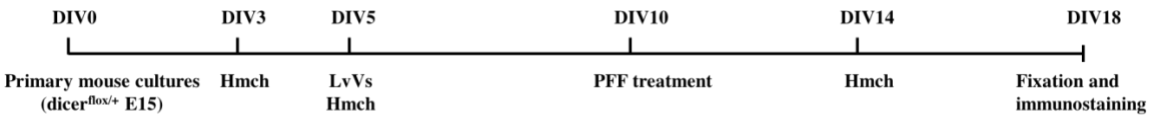

Figure 8 Experimental timeline of transductions, PFF treatments and endpoints. Primary cortical cultures were derived from E15 *Dicer* $^{flox/+}$ mouse embryos that were transduced with lenti-hSYN-GFP-T2A-Cre on DIV5 to achieve *Dicer*^{HET} knockout cultures. Part of the cultures were infected with lenti-hSYN-T2A-GFP LvVs to serve as a vector control in the experiment. PFFs were applied to the cultures 5 days post-transduction

(DIV10) and were induced for 7 days. PFF treatment was applied to half of the plate, which consisted of untransduced, lenti-hSYN-T2A-GFP- transduced or lenti-hSYN-GFP-T2A-Cre-transduced cultures. For more details see materials and methods.

5.2.1 Assessing vulnerability of *Dicer*^{HET} primary cortical neurons

The number of neurons in the cultures were counted by utilizing two nuclear labels: DAPI stain, binding to cellular DNA and capturing all cell nuclei, and NeuN immunohistochemical stain that specifically marks neuronal nuclei by binding to a nuclear protein present in vast majority of neurons. The results of the analysis, presented in Figure 9, showed that there was little difference between different groups. First, transduction with neither vector affected cell survival adversely, as evident by comparison between the groups not treated with PFFs (Figure 9A). This also implies that the heterozygous *Dicer* deletion did not influence survival. Second, we observed that PFFs did not induce increased apoptosis, as no apparent neuronal loss could be detected after 7 days of PFF induction (Figure 9B). More importantly, we did not observe significant difference between the treated groups either (Figure 9B). Altogether, these results indicate that *Dicer*^{HET} genotype did not confer cultured primary cortical neurons a greater vulnerability under PFF-induced stress conditions.

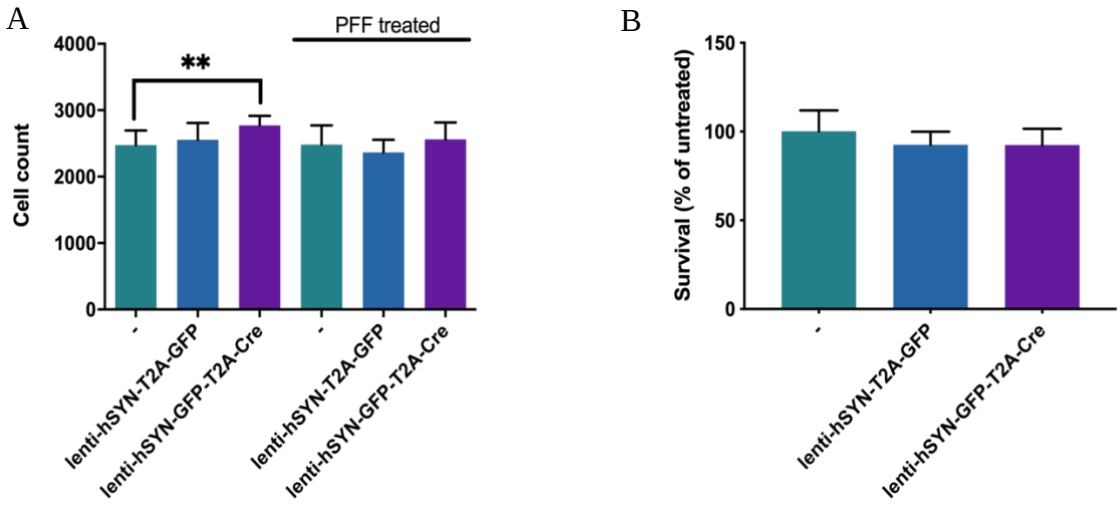

Figure 9 Assessing vulnerability of primary cortical cultures to PFF treatment. Cell counts were assessed 12 days post transduction and 7 days post PFF treatment (2.5 ng/µl)

(as described in Figure 8), using quantitative image analysis based on nuclear counterstaining with DAPI and NeuN antibody. A-B) Cell counts did not present significant variation between different groups, suggesting neither transductions nor PFF treatment impacted vulnerability of the neurons adversely. The error bars indicate mean ±SD of 4 replicates (or 10 for untreated control); statistically significant differences in mean were determined using one-way ANOVA coupled with multiple comparison correction using uncorrected Fisher's least significant difference (LSD). ** denotes statistical significance ($p < 0.01$).

5.2.2 αSyn aggregation may be increased in *Dicer*^{HET} primary cortical cultures

Most of the aggregating form of αSyn is hyperphosphorylated at serine 129 (Ser129) (Fujiwara et al., 2002; Luk et al., 2012). Therefore, we performed immunofluorescence staining with antibodies that specifically target phosphorylated (at Ser129) form of αSyn (pSer129-αSyn), in order to visualize the PFF-seeded aggregates. All the PFF-treated cultures exhibited αSyn pathology, as evident by extensive and intense immunostaining of pSer129-αSyn-positive aggregates (Figure 10). Aggregates were observed in neuronal somata and along neurites, where they formed accumulations resembling small puncta to larger LB-like and LN-like filaments (Figure 10). Control groups unexposed to PFFs did not show positive signal for pSer129-αSyn (Figure 11A first panel from left).

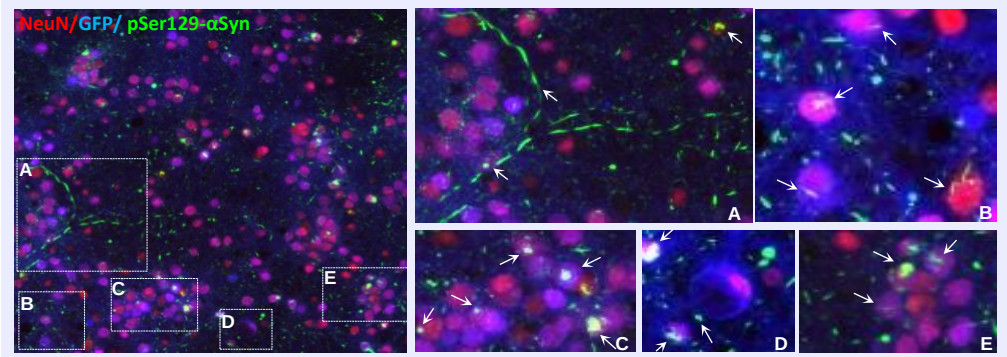

Figure 10 Immunofluorescence of aggregated αSyn in primary cortical cultures. To seed αSyn aggregation, cells were treated with PFFs and incubated for 7 days. Aggregates were visualized by immunohistochemical stain targeting Serine 129 Phosphorylation on αSyn. pSer129-αSyn-positive aggregates were observed in all PFF-treated cultures. Aggregates exhibited various shapes and sizes and appeared in neuronal somata

(immunostained with NeuN antibody) and along neurites. Arrows point to various morphological structures of the pSer129-αSyn-positive accumulations, such as globular or tread-like aggregates resembling LB inclusions or filaments and serpentine-like aggregates resembling LNs. Scale bar, 50 µm. NeuN = Neuronal nuclei, DAPI = 4',6-diamidino-2-phenylindole, pSer129-αSyn = phosphorylated αSyn at residue Ser129.

The number of neurons exhibiting pSer129-αSyn pathology (in the somata) were determined by counting the number of NeuN-positive cells colocalized with LB-like pSer129-αSyn-positive aggregates. The results, as shown in Figure 11B, indicate that *Dicer*^{HET} cultures (lenti-hSYN-GFP-T2A-Cre) had a greater accumulation of pSer129-αSyn aggregates. However, the difference reached statistical significance only in comparison with the transduction control (-). The observed difference between vector control (lenti-hSYN-T2A-GFP) and *Dicer*^{HET} was not significant. We also investigated the signal intensity and size of the LB-like aggregates present in neuronal soma. Interestingly, we found that pSer129-αSyn staining was more pronounced in *Dicer*^{HET} neurons (Figure 11C). However, again, the result was statistically significant only against one of the controls. Furthermore, we did not find a statistically meaningful trend in size differences (Figure 11D).

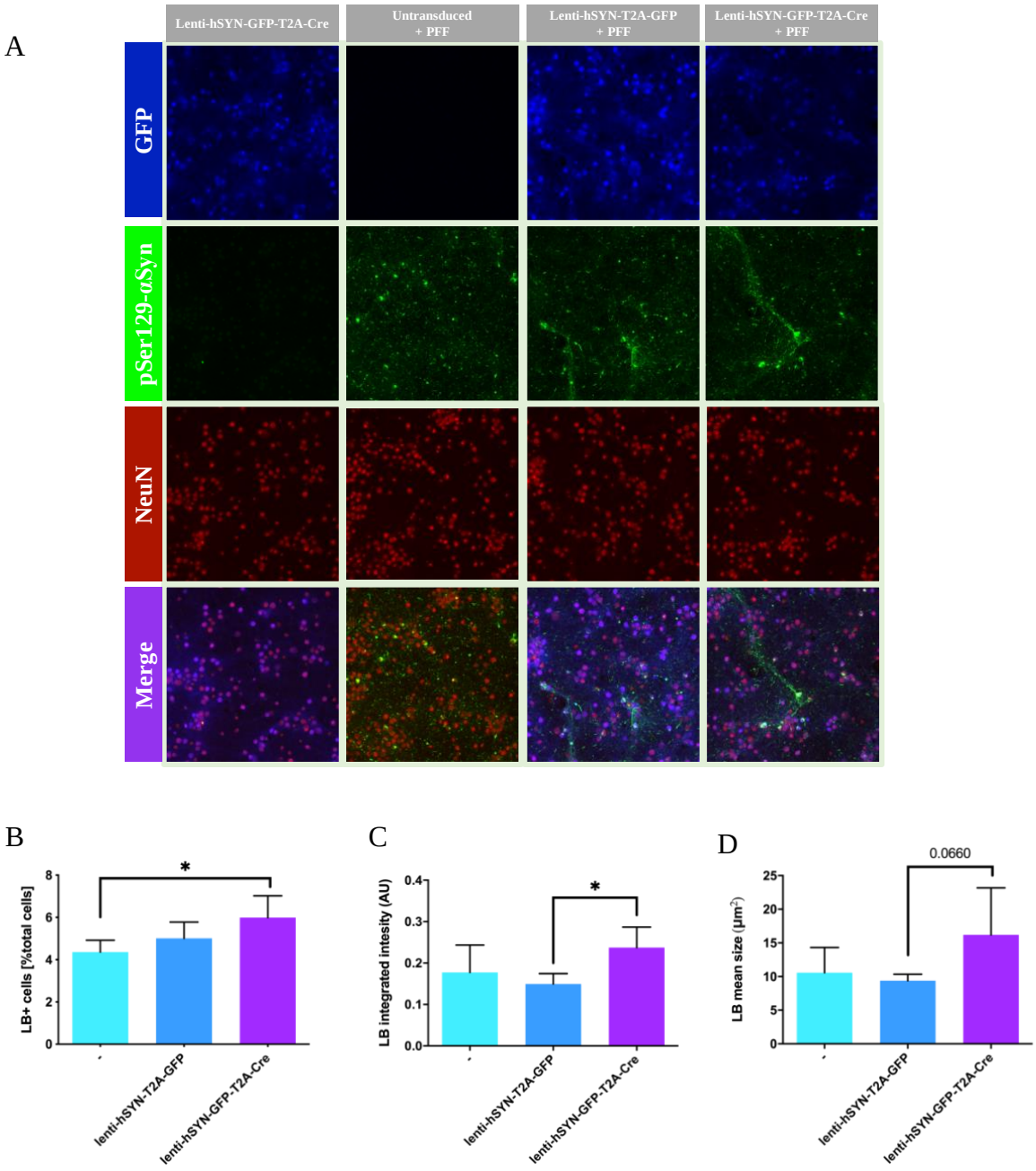

Figure 11 Susceptibility of cultured *Dicer*^{HET} cortical neurons to formation of pSer129-αSyn-positive LB-like aggregates upon external PFF application. Primary cortical cultures were transduced with LvVs and treated with PFFs as described in Figure 8. A) Representative images of the cultures. pSer129-αSyn-positive aggregates, assessed by immunofluorescent staining, were detected in all PFF-treated cultures. pSer129-αSyn immunoreactivity was absent in the control groups unexposed to PFFs (left panel). Scale bars, 50 µm. B) Quantitative analysis of the NeuN-positive cells containing pSer129-αSyn-positive LB-like aggregates. *Dicer*^{HET} cultures (lenti-hSYN-GFP-T2A-Cre) had a higher number of cells with LB-like aggregates than the control cultures (-). The difference with the vector control (lenti-hSYN-T2A-GFP) was statistically non-significant. C) Mean

integrated fluorescence intensity of pSer129-αSyn-positive LB-like aggregates colocalized with the neuronal nuclei (NeuN)-positive somata. LB-like aggregates exhibited increased fluorescence intensity within the *Dicer*^{HET} neurons. In this case, meaningful difference was observed only in comparison with the vector control (lenti-hSYN-T2A-GFP). D) Mean size of pSer129-αSyn-positive aggregates within the NeuN-positive somata. Some difference with size of aggregates could be observed, however there was no statistically reliable trend. The error bars indicate mean ±SD of independent counts; statistical analysis was performed using one-way ANOVA with multiple comparison correction; * denotes statistical significance ($p < 0.05$). NeuN = Neuronal nuclei, DAPI = 4',6-diamidino-2-phenylindole, pSer129-αSyn = phosphorylated αSyn at residue Ser129, PFF = preformed fibrils.

6 Discussion

In this study, we set out to establish and validate a new approach to generate the *Dicer*^{HET} model *in vitro*. The model is based on heterozygous knockout of the *Dicer* gene and has been earlier proposed as a suitable genetic model for studying the relationship between disrupted miRNA biogenesis and neurodegeneration in the context of Parkinson's disease research (Chmielarz et al., 2017). For future convenience, we validated an approach based on conventional *Cre/loxP* system and lentiviral Cre delivery to generate the genetic knockouts in culture. In addition, we applied the model in a preliminary experiment to explore the association between Dicer function with progression of Lewy pathology.

6.1 Validation of the *Dicer*^{HET} model

The method we implanted consist of generating *Dicer*$^{flox/+}$ primary cortical cultures that are transduced with lenti-hSYN-T2A-Cre vectors for Cre expression. We demonstrated that lenti-hSYN-GFP-T2A-Cre vectors produce fully functional and effective lentiviral particles that can induce efficient recombination of the *Dicer* allele flanked by *loxP* sites (floxed). The transduction event itself did not seem to increase vulnerability in the cultures. Our data showed that the best recombination efficiency was achieved when cultures (derived from E15 mouse embryos) were exposed to 0.5 µl of viral preparation between 5 to 12 days *in vitro* (DIV). Under these experimental settings, knockout of the floxed *Dicer* gene was evident after only 2 days and reached maximal efficiency after 5 days of incubation. Such

short induction time is a particularly beneficial feature as by default primary neuronal cells are not immortal in culture and allow a limited time for experimentation. Moreover, recombination efficiency seemed to be independent on the timing of the transduction; maximal gene editing event was observed in most cultures that were transduced between DIV5-12. This result was unexpected, since transduction efficiency is believed to decrease as neuronal cultures age (Wanisch et al., 2013). This is however a promising outcome, as older cultures provide access to neurons that have reached a more mature state (Beckh et al., 1989; Moody and Bosma, 2005; Gold et al., 2007; Okaty et al., 2009) and are for that reason better suited for PD-related experimentation. Unfortunately, we were unable to get satisfactory results in case of cultures that were transduced at later time points (DIV16-DIV21). Experiments with these cultures were however conducted under different conditions, and it seems possible that low recombination efficiency was due to lower titre of the virus. A further investigation, which takes this variable into account, was not undertaken in this work, owing to the labor intensity of the procedures and the limited time we had reserved for the project. Future studies are however recommended to establish the method for older cultures, as the ability to obtain *in vitro* systems that allow access to mature neurons holds a particular significance for PD and other aging related diseases.

The appeal of the *Dicer*^{HET} model is based on the premise that heterozygous deletion of the *Dicer* gene is translated into an efficient depletion of the Dicer protein. The existence of this connection has so far been based on a plausible conjecture, which has never been verified by direct examination. It is extremely unfortunate that in this study, despite of our efforts we weren't able to support this relationship either. Due to technical challenges, we weren't able to demonstrate Dicer downregulation at neither transcriptional nor translational level. Addressing this question is obviously an essential prerequisite for the future use of the model. In addition, it is also important to determine the time point at which efficient protein depletion is achieved, in order to fully establish the method.

6.2 Studying αSyn propagation in the *Dicer*^{HET} model

Next, we used the established culture system to investigate whether partial *Dicer* knockout could impact the extent of Lewy pathology. The main feature of this condition is abnormal

aggregation of presynaptic protein αSyn (Duda et al., 2002). Hence, we adopted a model that uses preformed fibrils (PFFs) to trigger αSyn aggregation (Luk et al., 2009; Volpicelli-Daley et al., 2011; Luk et al., 2012). Previous studies that have characterized this method have demonstrated that cultured primary neurons develop LB-like pathology upon PFF exposure and exhibit increased vulnerability which presumably emerges from toxic burden associated with αSyn aggregation (Volpicelli-Daley et al., 2011; Dryanovski et al., 2013; Volpicelli-Daley et al., 2014; Tapias et al., 2017). Moreover, in PD, Lewy pathology also affects neuronal populations outside SNpc, such as hippocampal and cortical neurons, as in our cultures (Duda et al., 2004; Duda et al., 2010). Consistent with earlier findings (Volpicelli-Daley et al., 2011; Volpicelli-Daley et al., 2014), we observed abundant presence of αSyn-positive aggregates in all the seeded cultures 7 days after the PFF application. In terms of histological features, the results match those observed in earlier studies (Volpicelli-Daley et al., 2011; Volpicelli-Daley et al., 2014). Most noticeable morphological structures of the aggregates included round LB-like and LN-like formations, which were distributed across all neuronal compartments. Regarding toxicity, we did not detect any evidence for increased vulnerability in the PFF-treated cultures after 7 days of incubation. This result also accords with earlier studies, which have reported effects of toxicity to first manifest at 14 days from PFF application (Volpicelli-Daley et al., 2011; Volpicelli-Daley et al., 2014; Tapias et al., 2017). Moreover, a recent study demonstrated that αSyn aggregation does not cause significant cellular dysfunction nor triggers cell death until first cytoplasmic LB inclusions begin to form, which was reported to occur from 14 days post PFF seeding onward (Mahul-Mellier et al., 2020).

An interesting observation to emerge from our investigation was that αSyn aggregation was slightly increased in the *Dicer*^{HET} cultures. However, statistical tests revealed that the observed differences were non-significant against both control groups simultaneously (non-transduced or vector control). In theory, however, such outcome seems likely, since disturbed miRNA processing (as a result of Dicer downregulation) can contribute to various pathogenic phenotypes (Radhakrishnan and Alwin, 2016). Even though the causes of αSyn aggregation still remain a topic of debate, the relevance of miRNAs in αSyn regulation are clearly supported by the current findings (Zhao and Wang, 2019). For example, a number of miRNAs, such as miR-7, miR-153, miR-34b, miR-34c and miR-214 have been found to directly target αSyn (Junn et al., 2009; Doxakis, 2010; Kabaria et al., 2015; Wang et al., 2015). A number of other miRNAs have been reported to regulate

cellular machinery involved in removal of aggregated αSyn (Alvarez-Erviti et al., 2013; Li et al., 2014; Zhang and Cheng, 2014). Thereby, miRNA deregulation by means of lowered Dicer activity could increase endogenous αSyn levels while in parallel, disturb mechanisms that clear aggregated αSyn proteins. Indeed, altering Dicer activity would affect a much more complex network of interactions. Dicer not only functions as a regulator of global miRNA levels, but also has miRNA independent non-canonical roles (Burger and Gullerova, 2015). Perturbation of any of these biological functions could initiate a cascade of molecular events that alter cellular homeostasis and trigger various pathogenic mechanisms. By all means, it is reasonable to assume that lowered Dicer activity could promote increased αSyn aggregation. With longer incubation times increased αSyn build-up of *Dicer*^{HET} cultures may be even more pronounced and definite. This may also ultimately contribute to increased vulnerability of the cultures as well. A future study is therefore recommended to assess the effects of PFF-induced αSyn aggregation on the *Dicer*^{HET} cultures over longer time frames.

7 Conclusions

Herein, we report of a validated *Dicer*^{HET} *in vitro* model produced from primary mouse cortical cultures with a fast, efficient and reproducible approach. Biochemical and imaging analyses allowed us to identify optimal parameters within our experimental setup and demonstrate that the model is suitable for relevant practical applications. The data obtained in this study could be of high value in the future use of the model. Further validation is however required to establish better and more detailed guidelines for the method and to characterize the model. Most importantly, a protein analysis of Dicer is strongly recommended to include future investigation. Nevertheless, the convenience of the lentiviral approach we applied is that it reduces the time, costs, labor and number of animals needed for producing genetic knockout in comparison to methods that depend on traditional breeding schemes. Additionally, since Dicer has a crucial role during the early stages of development, this approach provides a unique way to ensure that normal development of the cells is not hampered in the parental tissues. In conclusion, our data suggest that after sufficient characterization, the *Dicer*^{HET} model will be a suitable *in vitro* system to study pathological consequences of dysregulated miRNA biogenesis machinery. Research efforts that address this intriguing relationship may lead to findings that have

important implications for elucidating neurobiological basis of PD and developing a novel therapy.

8 Acknowledgments

I would like to express my gratitude to my master thesis advisor Prof. Teemu Teeri, who encouraged me and guided me and without whom I would not have been able to complete this process. I appreciate his valuable feedback and comments!

I would also like to thank my supervisor Dr. Andrii Domanskyi for giving me a great chance to explore a new area, where I could apply and master my skills, as well as for being so encouraging, supportive, and motivating. I am very grateful for generous help I received from Dr. Piotr Chmielarz and would like to thank him for all long and profound discussions that we had, be that about science, ethics, or anything else. He has always addressed any concerns that I had, was a true mentor and a role model for me.

I would also like to express my very profound gratitude to my parents, who shaped me into who I am personally and professionally. They have contributed so much to my interests and made science an integral part of my life and a subject to be passionate about since my early age. Especially I would like to thank my dad who has introduced me to the fascinating world of math and natural sciences.

Finally, I would like to acknowledge three very special lab rats Coco, Ruby and Luna, who luckily became my most beloved pets. These beautiful, intelligent and sophisticated creatures, capable of so many emotions and compassion, have taught me to appreciate and value their existence so much. Thus, I would like to salute all rats, mice and other lab animals in the world who bring the biggest sacrifice for the sake of our progress and researches. I hope everyone from the scientific community will value their lives and sacrifice as much as I do.

9 References

Ahmadinejad, F., Mowla, S. J., Honardoost, M. A., Arjenaki, M. G., Moazeni-Bistgani, M., Kheiri, S. & Teimori, H. 2017. Lower expression of miR-218 in human breast cancer is associated with lymph node metastases, higher grades, and poorer prognosis. Tumour biology: the journal of the International Society for Oncodevelopmental Biology and Medicine 39 (8): 1010428317698362.

Alvarez-Erviti, L., Seow, Y., Schapira, A. H., Rodriguez-Oroz, M. C., Obeso, J. A. & Cooper, J. M. 2013. Influence of microRNA deregulation on chaperone-mediated autophagy and α-synuclein pathology in Parkinson's disease. Cell death & disease 4 (3): e545.

Ambaw, A., Zheng, L., Tambe, M. A., Strathearn, K. E., Acosta, G., Hubers, S. A., Liu, F., Herr, S. A., Tang, J., Truong, A., Walls, E., Pond, A., Rochet, J. C. & Shi, R. 2018. Acrolein-mediated neuronal cell death and alpha-synuclein aggregation: implications for Parkinson's disease. Molecular and cellular neurosciences 88: 70–82.

Andersson, T., Rahman, S., Sansom, S. N., Alsiö, J. M., Kaneda, M., Smith, J., O'Carroll, D., Tarakhovsky, A. & Livesey, F. J. 2010. Reversible block of mouse neural stem cell differentiation in the absence of dicer and microRNAs. PloS one 5(10): e13453.

Anderson, J. P., Walker, D. E., Goldstein, J. M., de Laat, R., Banducci, K., Caccavello, R. J., Barbour, R., Huang, J., Kling, K., Lee, M., Diep, L., Keim, P. S., Shen, X., Chataway, T., Schlossmacher, M. G., Seubert, P., Schenk, D., Sinha, S., Gai, W. P. & Chilcote, T. J. 2006. Phosphorylation of Ser-129 is the dominant pathological modification of alpha-synuclein in familial and sporadic Lewy body disease. The Journal of biological chemistry 281(40): 29739–29752.

Ascherio, A. & Schwarzschild, M. A. 2016. The epidemiology of Parkinson's disease: risk factors and prevention. The Lancet Neurology 15: 1257-1272.

Baba, Y., Markopoulou, K., Putzke, J.D., Whaley, N.R., Farrer, M.J., Wszolek, Z.K. & Uitti, R.J. 2006. Phenotypic commonalities in familial and sporadic Parkinson disease. Archives of neurology 63: 579–583.

Bartel, D. P. 2004. MicroRNAs: genomics, biogenesis, mechanism, and function. Cell 116: 281-297.

Bartel, D. P. 2009. MicroRNAs: Target Recognition and Regulatory Functions. Cell 136 (2): 215–233.

Beckh, S., Noda, M., Lübbert, H. & Numa, S. 1989. Differential regulation of three sodium channel messenger RNAs in the rat central nervous system during development. The EMBO journal 8 (12): 3611–3616.

Berezikov, E. 2011. Evolution of microRNA diversity and regulation in animals. Nature Reviews Genetics 12: 846–860.

Bernheimer, H., Birkmayer, W., Hornykiewicz, O., Jellinger, K. & Seitelberger. F. 1973. Brain dopamine and the syndromes of Parkinson and Huntington. Clinical, morphological and neurochemical correlations. Journal of the Neurological Sciences 20: 415-45.

Bernstein, E., Caudy, A. A., Hammond, S. M. & Hannon, G. J. 2001. Role for a bidentate ribonuclease in the initiation step of RNA interference. Nature 409: 363 – 366.

Bernstein, E., Kim, S. Y., Carmell, M. A., Murchison, E. P., Alcorn, H., Li, M. Z., Mills, A. A., Elledge, S. J., Anderson, K. V. & Hannon, G. J. 2003. Dicer is essential for mouse development. Nature genetics 35 (3): 215–217.

Billy, E., Brondani, V., Zhang. H., Muller, U. & Filipowicz, W. 2001. Specific interference with gene expression induced by long, double-stranded RNA in mouse embryonal teratocarcinoma cell lines. Proceedings of the National Academy of Sciences of the United States 98: 14428–14433.

Bracken, C.P., Scott, H.S. & Goodall, G.J. 2016. A network-biology perspective of microRNA function and dysfunctionin cancer. Nature Reviews Genetics 17: 719–732.

Broughton, J.P., Lovci, M.T., Huang, J.L., Yeo, G.W. & Pasquinelli, A.E. 2016. Pairing beyond the Seed Supports MicroRNA Targeting Specificity. Molecular Cell. 64: 320–33.

Burger, K. & Gullerova, M. 2015. Swiss army knives: non-canonical functions of nuclear Drosha and Dicer. Nature reviews. Molecular cell biology 16 (7): 417–430.

Cai, X., Hagedorn, C. H. & Cullen, B. R. 2004. Human microRNAs are processed from capped, polyadenylated transcripts that can also function as mRNAs. RNA 10 (12): 1957–1966.

Calin, G. A. & Croce, C. M. 2006. MicroRNA signatures in human cancers. Nature reviews. Cancer 6 (11): 857–866.

Cannon, J. R. & Greenamyre, J. T. 2013. Gene-environment interactions in Parkinson's disease: specific evidence in humans and mammalian models. Neurobiology of disease 57: 38–46.

Cao, D.D., Li, L. & Chan, W.Y. 2016. MicroRNAs: Key regulators in the central nervous system and their implication in neurological diseases. International Journal Of Molecular Sciences 17.

Carthew, R. W. & Sontheimer, E. J. 2009. Origins and Mechanisms of miRNAs and siRNAs. Cell 136: 642–655.

Cerutti, H. & Casas-Mollano, J. A. 2006. On the origin and functions of RNA-mediated silencing: from protists to man. Current genetics 50 (2): 81–99.

Chaudhuri, K. R., Healy, D. & Shapira, A. H. V. 2006. Non-motor symptoms of Parkinson's disease: Diagnosis and management. The Lancet. Neurology 5: 235–245.

Chaudhuri, R. K., Poewe, W. & Brooks, D. 2018. Motor and Nonmotor Complications of Levodopa: Phenomenology, Risk Factors, and Imaging Features. Movement disorders: official journal of the Movement Disorder Society 33 (6): 909–919.

Chen, L., Heikkinen, L., Wang, C., Yang, Y., Sun, H. & Wong, G. 2019a. Trends in the development of miRNA bioinformatics tools. Briefings in bioinformatics 20 (5): 1836–1852.

Chen, C., Turnbull, D. M. & Reeve, A. K. 2019b. Mitochondrial Dysfunction in Parkinson's Disease-Cause or Consequence? Biology, 8 (2): 38.

Chen, J. A. & Wichterle, H. 2012. Apoptosis of limb innervating motor neurons and erosion of motor pool identity upon lineage specific Dicer inactivation. Frontiers in neuroscience 6: 69.

Cho, K. H. T., Xu, B., Blenkiron, C. & Fraser, M. 2019. Emerging Roles of miRNAs in Brain Development and Perinatal Brain Injury. Frontiers in Physiolgy 10: 227.

Chuang, J. & Jones, P. Epigenetics and MicroRNAs. 2007. Pediatric Research 61: 24–29.

Collier, T. J., Kanaan, N. M. & Kordower, J. H. 2011. Ageing as a primary risk factor for Parkinson's disease: evidence from studies of non-human primates. Nature Reviews Neuroscience 12: 359–366.

Cuellar, T. L., Davis, T. H., Nelson, P. T., Loeb, G. B., Harfe, B. D., Ullian, E. & McManus, M. T. 2008. Dicer loss in striatal neurons produces behavioral and neuroanatomical phenotypes in the absence of neurodegeneration. Proceedings of the National Academy of Sciences of the United States of America 105 (14): 5614–5619.

Dauer, W. & Przedborski, S. 2003. Parkinson's disease: mechanisms and models. Neuron 39: 889–909.

Davis, T. H., Cuellar, T. L., Koch, S. M., Barker, A. J., Harfe, B. D., McManus, M. T. & Ullian, E. M. 2008. Conditional loss of Dicer disrupts cellular and tissue morphogenesis in the cortex and hippocampus. The Journal of neuroscience: the official journal of the Society for Neuroscience 28 (17): 4322–4330.

Davis, G. M., Haas, M. A. & Pocock, R. 2015. MicroRNAs: Not "Fine-Tuners" but Key Regulators of Neuronal Development and Function. Frontiers in neurology 6: 245.

de Lau, L. M. & Breteler, M. M. 2006. Epidemiology of Parkinson's disease. The Lancet Neurology 5 (6): 525–35.

De Pietri Tonelli, D., Pulvers, J. N., Haffner, C., Murchison, E. P., Hannon, G. J. & Huttner, W. B. 2008. miRNAs are essential for survival and differentiation of newborn neurons but not for expansion of neural progenitors during early neurogenesis in the mouse embryonic neocortex. Development 135 (23): 3911–3921.

De Pietri Tonelli, D., Clovis, Y. M. & Huttner, W. B. 2014. Detection and monitoring of microRNA expression in developing mouse brain and fixed brain cryosections. Methods in molecular biology (Clifton, N.J.) 1092: 31–42.

de Jong, D., Eitel, M., Jakob, W., Osigus, H. J., Hadrys, H., Desalle, R. & Schierwater, B. 2009. Multiple dicer genes in the early-diverging metazoa. Molecular biology and evolution 26(6): 1333–1340.

de Rie, D., Abugessaisa, I., Alam, T., Arner, E., Arner, P., Ashoor, H., Åström, G., Babina, M., Bertin, N., Burroughs, A. M., Carlisle, A. J., Daub, C. O., Detmar, M., Deviatiiarov, R., Fort, A., Gebhard, C., Goldowitz, D., Guhl, S., Ha, T. J., Harshbarger, J., Hasegawa, A., Hashimoto, K., Herlyn, M., Heutink, P., Hitchens, K.J., Hon, C.C., Huang, E., Ishizu, Y., Kai, C., Kasukawa, T., Klinken, P., Lassmann, T., Lecellier, C.H., Lee, W., Lizio, M., Makeev, V., Mathelier, A., Medvedeva, Y.A., Mejhert, N., Mungall, C.J., Noma, S., Ohshima, M., Okada-Hatakeyama, M., Persson, H., Rizzu, P., Roudnicky, F., Sætrom, P., Sato, H., Severin, J., Shin, J.W., Swoboda, R.K., Tarui, H., Toyoda, H., Vitting-Seerup, K., Winteringham, L., Yamaguchi, Y., Yasuzawa, K., Yoneda, M., Yumoto, N., Zabierowski, S., Zhang, P.G., Wells, C.A., Summers, K.M., Kawaji, H., Sandelin, A., Rehli, M., Hayashizaki, Y., Carninci, P., Forrest, A.R.R. & de Hoon, M. 2017. An integrated expression atlas of miRNAs and their promoters in human and mouse. Nature biotechnology 35 (9): 872–878.

Deng, S., Calin, G. A., Croce, C. M., Coukos, G. & Zhang, L. 2008. Mechanisms of microRNA deregulation in human cancer. Cell cycle 7 (17): 2643–2646.

Di Monte, D. A., Lavasani, M. & Manning-Bog, A. B. 2002. Environmental factors in Parkinson's disease. Neurotoxicology 23: 487–502.

Dimmeler, S. & Nicotera, P. 2013. MicroRNAs in age-related diseases. EMBO Molecular Medicine 5 (2): 180-190.

Dogini, D. B., Pascoal, V. D., Avansini, S. H., Vieira, A. S., Pereira, T. C. & Lopes-Cendes, I. 2014. The new world of RNAs. Genetics and molecular biology 37 (1 Suppl): 285–293.

Doxakis, E. 2010. Post-transcriptional regulation of alpha-synuclein expression by mir-7 and mir-153. The Journal of biological chemistry 285 (17): 12726–12734.

Doyle, M., Jaskiewicz, L. & Filipowicz, W. 2012. Dicer proteins and their role in gene silencing pathways. The enzymes (ed. F Guo) 32: 1–35.

Duda, J. E. 2004. Pathology and neurotransmitter abnormalities of dementia with Lewy bodies. Dementia and geriatric cognitive disorders 17: 3–14.

Duda, J. E. 2010. Olfactory system pathology as a model of Lewy neurodegenerative disease. Journal of the neurological sciences 289: 49–54.

Duda, J. E., Giasson, B. I., Mabon, M. E., Lee, V. M. & Trojanowski, J. Q. 2002. Novel antibodies to synuclein show abundant striatal pathology in Lewy body diseases. Annals of neurology 52: 205–210.

Dryanovski, D. I., Guzman, J. N., Xie, Z., Galteri, D. J., Volpicelli-Daley, L. A., Lee, V. M., Miller, R. J., Schumacker, P. T. & Surmeier, D. J. 2013. Calcium entry and α-synuclein inclusions elevate dendritic mitochondrial oxidant stress in DA neurons. The Journal of neuroscience: the official journal of the Society for Neuroscience 33 (24): 10154–10164.

Driver, J. A., Logroscino, G., Gaziano, J. M. & Kurth, T. 2009. Incidence and remaining lifetime risk of Parkinson disease in advanced age. Neurology 72: 432–438.

Emde, A., Eitan, C., Liou, L. L., Libby, R. T., Rivkin, N., Magen, I., Reichenstein, I., Oppenheim, H., Eilam, R., Silvestroni, A., Alajajian, B., Ben-Dov, I. Z., Aebischer, J., Savidor, A., Levin, Y., Sons, R., Hammond, S. M., Ravits, J. M., Möller, T. & Hornstein, E. 2015. Dysregulated miRNA biogenesis downstream of cellular stress and ALS-causing mutations: a new mechanism for ALS. The EMBO journal 34 (21): 2633–2651.

Emde, A. & Hornstein, E. 2014. miRNAs at the interface of cellular stress and disease. The EMBO journal 33 (13): 1428–1437.

Esteller, M. 2011. Non-coding RNAs in human disease. Nature Reviews Genetics 12 (12): 861.

Fasano, A., Daniele, A. & Albanese, A. 2012. Treatment of motor and non-motor features of Parkinson's disease with deep brain stimulation. The Lancet. Neurology 11 (5): 429–442.

Feil, R., Wagner, J., Metzger, D. & Chambon, P. 1997. Regulation of Cre recombinase activity by mutated estrogen receptor ligand-binding domains. Biochemical and biophysical research communications 237 (3): 752–757.

Fire, A., Xu, S., Montgomery, M. K., Kostas, S. A., Driver, S. E. & Mello, C. C. 1998. Potent and specific genetic interference by double-stranded RNA in *Caenorhabditis elegans*. Nature 391 (6669): 806–811.

Fox, S. H., Katzenschlager, R., Lim, S. Y., Ravina, B., Seppi, K., Coelho, M., Poewe, W., Rascol, O., Goetz, C. G. & Sampaio, C. 2011. The Movement Disorder Society Evidence-Based Medicine

Review Update: Treatments for the motor symptoms of Parkinson's disease. Movement disorders: official journal of the Movement Disorder Society 26 Suppl 3: S2–S41.

Friedman, R. C., Farh, K. K., Burge, C. B. & Bartel, D. P. 2009. Most mammalian mRNAs are conserved targets of microRNAs. Genome research 19(1): 92–105.

Fu, G., Brkic, J., Hayder, H. & Peng, C. 2013. MicroRNAs in Human Placental Development and Pregnancy Complications. International Journal of Molecular Sciences 14 (3): 5544.

Fujiwara, H., Hasegawa, M., Dohmae, N., Kawashima, A., Masliah, E., Goldberg, J., KojI, S., TakeshI, T. & Iwatsubo, H. 2002. alpha -Synuclein is phosphorylated in synucleinopathy lesions. Nature Cell Biology 4 (2): 160-164.

Gardiner, E., Beveridge, N. J., Wu, J. Q., Carr, V., Scott, R. J., Tooney, P. A. & Cairns, M. J. 2012. Imprinted DLK1-DIO3 region of 14q32 defines a schizophrenia-associated miRNA signature in peripheral blood mononuclear cells. Molecular psychiatry 17 (8): 827–840.

GBD 2016 Parkinson's Disease Collaborators. 2018. Global, regional, and national burden of Parkinson's disease, 1990-2016: a systematic analysis for the Global Burden of Disease Study 2016. The Lancet. Neurology 17 (11): 939–953.

Gehrke, S., Imai, Y., Sokol, N. & Lu, B. 2010. Pathogenic LRRK2 negatively regulates microRNA-mediated translational repression. Nature 466 (7306): 637.

Georgi, S. A. & Reh, T. A. 2010. Dicer is required for the transition from early to late progenitor state in the developing mouse retina. The Journal of neuroscience: the official journal of the Society for Neuroscience 30 (11): 4048–4061.

Giraldez, A. J., Cinalli, R. M., Glasner, M. E., Enright, A. J., Thomson, J. M., Baskerville, S., Hammond, S. M., Bartel, D. P. & Schier, A. F. 2005. MicroRNAs regulate brain morphogenesis in zebrafish. Science 308 (5723): 833–838.

Goh, S. Y., Chao, Y. X., Dheen, S. T., Tan, E. K. & Tay, S. S. 2019. Role of MicroRNAs in Parkinson's Disease. International journal of molecular sciences 20 (22): 5649.

Goker-Alpan, O., Stubblefield, B. K., Giasson, B. I. & Sidransky, E. 2010. Glucocerebrosidase is present in α-synuclein inclusions in Lewy body disorders. Acta neuropathologica 120 (5): 641–649.

Gold, C., Henze, D. A. & Koch, C. 2007. Using extracellular action potential recordings to constrain compartmental models. Journal of computational neuroscience 23 (1): 39–58.

Gregory, R. I., Yan, K. P., Amuthan, G., Chendrimada, T., Doratotaj, B., Cooch, N. & Shiekhattar, R. 2004. The Microprocessor complex mediates the genesis of microRNAs. Nature 432 (7014): 235–240.

Griffiths-Jones, S. 2004. The microRNA Registry. Nucleic acids research 32: D109–D111.

Griffiths-Jones, S., Saini, H. K., Van Dongen, S. & Enright, A. J. 2008. miRBase: Tools for microRNA genomics. Nucleic acids research 36 (Database issue): D154.

Grishok, A., Pasquinelli, A. E., Conte, D., Li, N., Parrish, S., Ha, I., Baillie, D. L., Fire, A., Ruvkun, G. & Mello, C. C. 2001. Genes and mechanisms related to RNA interference regulate expression of the small temporal RNAs that control C. elegans developmental timing. Cell 106 (1): 23–34.

PD Med Collaborative Group: Gray, R., Ives, N., Rick, C., Patel, S., Gray, A., Jenkinson, C., McIntosh, E., Wheatley, K., Williams, A. & Clarke, C. E. 2014. Long-term effectiveness of dopamine agonists and monoamine oxidase B inhibitors compared with levodopa as initial treatment for Parkinson's disease (PD MED): a large, open-label, pragmatic randomised trial. Lancet 384 (9949): 1196–1205.

Guttman, M., Burkholder, J., Kish, S., Hussey, D., Wilson, A., Dasilva, J. & Houle, S. 1997. [C-11]RTI-32 PET studies of the dopamine transporter in early dopa-naive Parkinson's disease: Implications for the symptomatic threshold. Neurology 48 (6): 1578-1583.

Ha, M. & Kim, V. N. 2014. Regulation of microRNA biogenesis. Nature Reviews Molecular Cell Biology 15 (8).

Hanna, J., Hossain, G. S. & Kocerha, J. 2019. The Potential for microRNA Therapeutics and Clinical Research. Frontiers in genetics 10: 478.

Harfe, B. D., McManus, M. T., Mansfield, J. H., Hornstein, E. & Tabin, C. J. 2005. The RNaseIII enzyme Dicer is required for morphogenesis but not patterning of the vertebrate limb. Proceedings of the National Academy of Sciences of the United States of America 102 (31): 10898–10903.

Hayes, J., Peruzzi, P. P. & Lawler, S. 2014. MicroRNAs in cancer: Biomarkers, functions and therapy. Trends in Molecular Medicine 20 (8): 460-469.

He, X., Zhang, Q., Liu, Y. & Pan, X. 2007. Cloning and identification of novel microRNAs from rat hippocampus. Acta biochimica et biophysica Sinica 39 (9): 708–714.

Heldt, S. A., Stanek, L., Chhatwal, J. P. & Ressler, K. J. 2007. Hippocampus-specific deletion of BDNF in adult mice impairs spatial memory and extinction of aversive memories. Molecular psychiatry 12 (7): 656–670.

Hinske, L. C., França, G. S., Torres, H. A., Ohara, D. T., Lopes-Ramos, C. M., Heyn, J., Reis, L. F., Ohno-Machado, L., Kreth, S. & Galante, P. A. 2014. miRIAD-integrating microRNA inter- and intragenic data. Database: the journal of biological databases and curation 2014: bau099.

Hinske, L. C. G., Galante, P. A. F., Kuo, W. P. & Ohno - Machado, L. 2010. A potential role for intragenic miRNAs on their hosts' interactome. BMC Genomics 11: 533.

Hong, J., Zhang, H., Kawase-Koga, Y. & Sun, T. 2013. MicroRNA function is required for neurite outgrowth of mature neurons in the mouse postnatal cerebral cortex. Frontiers in cellular neuroscience 7: 151.

Hornykiewicz, O. 1998. Biochemical aspects of Parkinson's disease. Neurology 51 (2 Suppl 2): S2–S9.

Hu, Z. & Li, Z. 2017. miRNAs in synapse development and synaptic plasticity. Current opinion in neurobiology 45: 24–31.

Huang, W. 2017. MicroRNAs: biomarkers, diagnostics, and therapeutics. Methods in Molecular Biology 1617: 57.

Huang, T., Liu, Y., Huang, M., Zhao, X. & Cheng, L. 2010. Wnt1-cre-mediated conditional loss of Dicer results in malformation of the midbrain and cerebellum and failure of neural crest and DA differentiation in mice. Journal of molecular cell biology 2 (3): 152–163.

Hébert, S. S., Papadopoulou, A. S., Smith, P., Galas, M. -. C., Planel, E., Silahtaroglu, A. N., Nicolas, S., Luc, B. & De Strooper, B. 2010. Genetic ablation of Dicer in adult forebrain neurons results in abnormal tau hyperphosphorylation and neurodegeneration. Human Molecular Genetics 19 (20): 3959-3969.

Ikeda, S., Kong, S. W., Lu, J., Bisping, E., Zhang, H., Allen, P. D., Golub, T. R., Pieske, B. & Pu, W. T. 2007. Altered microRNA expression in human heart disease. Physiological genomics 31 (3): 367–373.

Junn, E., Lee, K. W., Jeong, B. S., Chan, T. W., Im, J. Y. & Mouradian, M. M. 2009. Repression of alpha-synuclein expression and toxicity by microRNA-7. Proceedings of the National Academy of Sciences of the United States of America 106 (31): 13052–13057.

Kabaria, S., Choi, D. C., Chaudhuri, A. D., Mouradian, M. M. & Junn, E. 2015. Inhibition of miR-34b and miR-34c enhances α-synuclein expression in Parkinson's disease. FEBS letters 589 (3): 319–325.

Kai, K., Dittmar, R. L. & Sen, S. 2018. Secretory microRNAs as biomarkers of cancer. Seminars in cell & developmental biology 78: 22–36.

Kalia, L.V. & Lang, A.E. 2015. Parkinson's disease. Lancet 386 (9996): 896–912.

Kaneko, H., Dridi, S., Tarallo, V., Gelfand, B. D., Fowler, B. J., Cho, W. G., Kleinman, M. E., Ponicsan, S. L., Hauswirth, W. W., Chiodo, V. A., Karikó, K., Yoo, J. W., Lee, D. K., Hadziahmetovic, M., Song, Y., Misra, S., Chaudhuri, G., Buaas, F. W., Braun, R. E., Hinton, D. R., Zhang, Q., Grossniklaus, H.E., Provis, J.M., Madigan, M.C., Milam, A.H., Justice, N.L., Albuquerque, R.J., Blandford, A.D., Bogdanovich, S., Hirano, Y., Witta, J., Fuchs, E., Littman, D.R., Ambati, B.K., Rudin, C.M., Chong, M.M., Provost, P., Kugel, J.F., Goodrich, J.A., Dunaief, J.L., Baffi, J.Z. & Ambati, J. 2011. DICER1 deficit induces Alu RNA toxicity in age-related macular degeneration. Nature 471 (7338): 325–330.

Kanno, S., Nosho, K., Ishigami, K., Yamamoto, I., Koide, H., Kurihara, H., Mitsuhashi, K., Shitani, M., Motoya, M., Sasaki, S., Tanuma, T., Maguchi, H., Hasegawa, T., Kimura, Y., Takemasa, I., Shinomura, Y. & Nakase, H. 2017. MicroRNA-196b is an independent prognostic biomarker in patients with pancreatic cancer. Carcinogenesis 38 (4): 425–431.

Kawase-Koga, Y., Otaegi, G. & Sun, T. 2009. Different timings of Dicer deletion affect neurogenesis and gliogenesis in the developing mouse central nervous system. Developmental dynamics: an official publication of the American Association of Anatomists 238 (11): 2800–2812.

Ketting, R. F., Fischer, S. E., Bernstein, E., Sijen, T., Hannon, G. J. & Plasterk, R. H. 2001. Dicer functions in RNA interference and in synthesis of small RNA involved in developmental timing in C. elegans. Genes & development 15 (20): 2654–2659.

Kim, J., Inoue, K., Ishii, J., Vanti, W. B., Voronov, S. V., Murchison, E., Hannon, G. & Abeliovich, A. A. 2007. microRNA feedback circuit in midbrain dopamine neurons. Science 17: 1220-1224.

Kim, Y. K. & Kim, V. N. 2007. Processing of intronic microRNAs. The EMBO journal 26 (3): 775–783.

Klingelhoefer, L. & Reichmann, H. 2017. Parkinson's disease as a multisystem disorder. Journal of neural transmission 124 (6): 709–713.

Kobayashi, H. & Tomari, Y. 2016. RISC assembly: Coordination between small RNAs and Argonaute proteins. Biochimica et biophysica acta 1859 (1): 71–81.

Konopka, W., Kiryk, A., Novak, M., Herwerth, M., Parkitna, J. R., Wawrzyniak, M., Kowarsch, A., Michaluk, P., Dzwonek, J., Arnsperger, T., Wilczynski, G., Merkenschlager, M., Theis, F. J., Köhr, G., Kaczmarek, L. & Schütz, G. 2010. MicroRNA loss enhances learning and memory in mice. The Journal of neuroscience: the official journal of the Society for Neuroscience 30 (44): 14835–14842.

Kotaja, N., Bhattacharyya, S. N., Jaskiewicz, L., Kimmins, S., Parvinen, M., Filipowicz, W. & Sassone - Corsi, P. 2006. The chromatoid body of male germ cells: Similarity with processing bodies and presence of Dicer and microRNA pathway components. Proceedings of the National Academy of Sciences of the United States 103 (8): 2647.

Kozomara, A., Birgaoanu, M. & Griffiths-Jones, S. 2019. miRBase: from microRNA sequences to function. Nucleic acids research 47(D1): D155–D162.

Kumar, K. R., Djarmati-Westenberger, A. & Grünewald, A. 2011. Genetics of Parkinson's disease. Seminars in neurology 31 (5): 433–440.

Kye, M. J., Liu, T., Levy, S. F., Xu, N. L., Groves, B. B., Bonneau, R., Lao, K. & Kosik, K. S. 2007. Somatodendritic microRNAs identified by laser capture and multiplex RT-PCR. RNA 13 (8): 1224–1234.

Lagos-Quintana, M., Rauhut, R., Lendeckel, W. & Tuschl, T. 2001. Identification of novel genes coding for small expressed RNAs. Science 294 (5543): 853–858.

Lan, H., Lu, H., Wang, X. & Jin, H. 2015. MicroRNAs as potential biomarkers in cancer: opportunities and challenges. BioMed research international 2015: 125094.

Landgraf, P., Rusu, M., Sheridan, R., Sewer, A., Iovino, N., Aravin, A., Pfeffer, S., Rice, A., Kamphorst, A. O., Landthaler, M., Lin, C., Socci, N. D., Hermida, L., Fulci, V., Chiaretti, S., Foà, R., Schliwka, J., Fuchs, U., Novosel, A., Müller, R. U., Schermer, B., Bissels, U., Inman, J., Phan, Q., Chien, M., Weir, D.B., Choksi, R., De Vita, G., Frezzetti, D., Trompeter, H.I., Hornung, V., Teng, G., Hartmann, G., Palkovits, M., Di Lauro, R., Wernet, P., Macino, G., Rogler, C.E., Nagle, J.W., Ju, J., Papavasiliou, F.N., Benzing, T., Lichter, P., Tam, W., Brownstein, M.J., Bosio, A., Borkhardt, A., Russo, J.J., Sander, C., Zavolan, M. & Tuschl, T. 2007. A mammalian microRNA expression atlas based on small RNA library sequencing. Cell 129 (7): 1401–1414.

Lee, Y., Ahn, C., Han, J., Choi, H., Kim, J., Yim, J., Lee, J., Provost, P., Radmark, O., Kim, S. & Kim, V. N. 2003. The nuclear RNase III Drosha initiates microRNA processing. Nature 425 (6956): 415.

Lee, R. C., Feinbaum, R. L. & Ambros, V. 1993. The C. elegans heterochronic gene lin-4 encodes small RNAs with antisense complementarity to lin-14. Cell 75 (5): 843-854.

Lee, Y., Kim, M., Han, J., Yeom, K. H., Lee, S., Baek, S. H. & Kim, V. N. 2004a. MicroRNA genes are transcribed by RNA polymerase II. The EMBO journal 23 (20): 4051–4060.

Lee, Y. S., Nakahara, K., Pham, J. W., Kim, K., He, Z., Sontheimer, E. J. & Carthew, R. W. 2004b. Distinct Roles for Drosophila Dicer-1 and Dicer-2 in the siRNA/miRNA Silencing Pathways. Cell 117 (1): 69-81.

The Lewin Group, Inc., Economic Burden and Future Impact of Parkinson's Disease: final report. Available online:

https://www.michaeljfox.org/sites/default/files/media/document/2019%20Parkinson%27s%20Economic%20Burden%20Study%20-%20FINAL.pdf. Published on 2019, last accessed on 1.6.2020.

LeWitt, A. & Fahn, A. 2016. Levodopa therapy for Parkinson disease: A look backward and forward. Neurology 86: S3-S12.

Li, Q., Bian, S., Hong, J., Kawase-Koga, Y., Zhu, E., Zheng, Y., Yang, L. & Sun, T. 2011. Timing specific requirement of microRNA function is essential for embryonic and postnatal hippocampal development. PloS one 6 (10): e26000.

Li, G., Yang, H., Zhu, D., Huang, H., Liu, G. & Lun, P. 2014. Targeted suppression of chaperone-mediated autophagy by miR-320a promotes α-synuclein aggregation. International journal of molecular sciences 15 (9): 15845–15857.

Liang, H., Hippenmeyer, S. & Ghashghaei, H. T. 2012. A Nestin-cre transgenic mouse is insufficient for recombination in early embryonic neural progenitors. Biology open 1 (12): 1200–1203.

Lin, S. & Gregory, R.I. 2015. MicroRNA biogenesis pathways in cancer. Nature Reviews Cancer 15: 321–333.

Lill, C. M. 2016. Genetics of Parkinson's disease. Molecular and Cellular Probes 30 (6): 386-396.

Lu, J., Getz, G., Miska, E. A., Alvarez-Saavedra, E., Lamb, J., Peck, D., Sweet-Cordero, A., Ebert, B. L., Mak, R. H., Ferrando, A. A., Downing, J. R., Jacks, T., Horvitz, H. R. & Golub, T. R. 2005. MicroRNA expression profiles classify human cancers. Nature 435 (7043): 834–838.

Lu, M., Kong, X., Wang, H., Huang, G., Ye, C. & He, Z. 2017. A novel microRNAs expression signature for hepatocellular carcinoma diagnosis and prognosis. Oncotarget 8 (5): 8775–8784.

Luk, K. C., Song, C., O'Brien, P., Stieber, A., Branch, J. R., Brunden, K. R., Trojanowski, J. Q. & Lee, V. M. 2009. Exogenous alpha-synuclein fibrils seed the formation of Lewy body-like intracellular inclusions in cultured cells. Proceedings of the National Academy of Sciences of the United States of America: 106 (47): 20051–20056.

Luk, K. C., Kehm, V. M., Zhang, B., O'brien, P., Trojanowski, J. Q. & Lee, V. M. 2012. Intracerebral inoculation of pathological α-synuclein initiates a rapidly progressive neurodegenerative α-synucleinopathy in mice. The Journal of Experimental Medicine 209 (5): 975-986.

Lukiw, W. J. 2007. Micro-RNA speciation in fetal, adult and Alzheimer's disease hippocampus. Neuroreport 18 (3): 297–300.

Lukiw, W.J. 2012. Evolution and complexity of micro RNA in the human brain. Frontiers in genetics 3: 166.

Lund, E., Güttinger, S., Calado, A., Dahlberg, J. E. & Kutay, U. 2004. Nuclear export of microRNA precursors. Science 303 (5654): 95.

Maciotta, S., Meregalli, M. & Torrente, Y. 2013. The involvement of microRNAs in neurodegenerative diseases. Frontiers in cellular neuroscience 7: 265.

Macrae, I. J., Zhou, K. & Doudna, J. A. 2007. Structural determinants of RNA recognition and cleavage by Dicer. Nature Structural & Molecular Biology 14 (10): 934.

Macrae, I. J., Zhou, K., Li, F., Repic, A., Brooks, A. N., Cande, W. Z, Adams, P.D. & Doudna, J.A. 2006. Structural basis for double-stranded RNA processing by Dicer. Science 311: 195–198.

Mahul-Mellier, A. L., Burtscher, J., Maharjan, N., Weerens, L., Croisier, M., Kuttler, F., Leleu, M., Knott, G. W. & Lashuel, H. A. 2020. The process of Lewy body formation, rather than simply α-synuclein fibrillization, is one of the major drivers of neurodegeneration. Proceedings of the National Academy of Sciences of the United States of America 117(9): 4971–4982.

Makeyev, E. V., Zhang, J., Carrasco, M. A. & Maniatis, T. 2007. The MicroRNA miR-124 promotes neuronal differentiation by triggering brain-specific alternative pre-mRNA splicing. Molecular cell 27 (3): 435–448.

Mclellan, M. A., Rosenthal, N. A. & Pinto, A. R. 2017. *Cre-loxP*-Mediated Recombination: General Principles and Experimental Considerations. Current protocols in mouse biology 7 (1): 1.

McLoughlin, H. S., Fineberg, S. K., Ghosh, L. L., Tecedor, L. & Davidson, B. L. 2012. Dicer is required for proliferation, viability, migration and differentiation in corticoneurogenesis. Neuroscience 223: 285–295.

Melo, C. A. & Melo, S. A. 2014. Biogenesis and physiology of microRNAs. Non-coding RNAs and Cancer 2: 5-24.

Mendell, J.T. 2012. Olson EN. MicroRNAs in stress signaling and human disease. Cell 148: 1172-1187.

Mercado, G., Valdés, P. & Hetz, C. 2013. An ER-centric view of Parkinson's disease. Trends in molecular medicine19 (3) :165–175.

Miñones-Moyano, E., Porta, S., Escaramís, G., Rabionet, R., Iraola, S., Kagerbauer, B., Espinosa-Parrilla, Y., Ferrer, I., Estivill, X. & Martí, E. 2011. MicroRNA profiling of Parkinson's disease brains identifies early downregulation of miR-34b/c which modulate mitochondrial function. Human molecular genetics 20 (15): 3067–3078.

Murphy, D., Dancis, B., Brown, J.R. 2008. The evolution of core proteins involved in microRNA biogenesis. BMC Evolutionary Biology 8: 92.

Moody, W. J. & Bosma, M. M. 2005. Ion channel development, spontaneous activity, and activity-dependent development in nerve and muscle cells. Physiological reviews 85 (3): 883–941.

Moisan, F., Kab, S., Mohamed, F., Canonico, M., Le Guern, M., Quintin, C., Carcaillon, L., Nicolau, J., Duport, N., Singh-Manoux, A., Boussac-Zarebska, M. & Elbaz, A. 2016. Parkinson disease male-to-female ratios increase with age: French nationwide study and meta-analysis. Journal of neurology, neurosurgery, and psychiatry 87 (9): 952–957.

Mori, M., Raghavan, P., Thomou, T., Boucher, J., Robida-Stubbs, S., Macotela, Y. & Kahn, C.R. 2012. Role of microRNA processing in adipose tissue in stress defense and longevity. Cell Metabolism 16 (3): 336–47.

Much, C., Auchynnikava, T., Pavlinic, D., Buness, A., Rappsilber, J., Benes, V., Allshire, R. & O'Carroll, D. 2016. Endogenous Mouse Dicer Is an Exclusively Cytoplasmic Protein. *PLoS genetics 12* (6): e1006095.

Mushtaq, G., Greig, N. H., Anwar, F., Zamzami, M. A., Choudhry, H., Shaik, M. M., Tamargo, I. A. & Kamal, M. A. 2016. miRNAs as Circulating Biomarkers for Alzheimer's Disease and Parkinson's Disease. Medicinal chemistry 12 (3): 217–225.

Nagy, A. 2000. Cre recombinase: The universal reagent for genome tailoring. Genesis 26 (2): 99-109.

Nigro, A., Menon, R., Bergamaschi, A., Clovis, Y. M., Baldi, A., Ehrmann, M., Comi, G., De Pietri Tonelli, D., Farina, C., Martino, G. & Muzio, L. 2012. MiR-30e and miR-181d control radial glia cell proliferation via HtrA1 modulation. Cell death & disease 3 (8): e360.

Nowakowski, T. J., Mysiak, K. S., Pratt, T. & Price, D. J. 2011. Functional Dicer is necessary for appropriate specification of radial glia during early development of mouse telencephalon. PloS one 6 (8): e23013.

Nowakowski, T. J., Rani, N., Golkaram, M., Zhou, H. R., Alvarado, B., Huch, K., West, J. A., Leyrat, A., Pollen, A. A., Kriegstein, A. R., Petzold, L. R. & Kosik, K. S. 2018. Regulation of cell-type-specific transcriptomes by microRNA networks during human brain development. Nature neuroscience 21 (12): 1784–1792.

O'Brien, J., Hayder, H., Zayed, Y. & Peng, C. 2018. Overview of MicroRNA Biogenesis, Mechanisms of Actions, and Circulation. Frontiers in endocrinology 9: 402.

Okaty, B. W., Miller, M. N., Sugino, K., Hempel, C. M. & Nelson, S. B. 2009. Transcriptional and electrophysiological maturation of neocortical fast-spiking GABAergic interneurons. Journal of Neuroscience 29: 7040–7052.

Palanichamy, J. K. & Rao, D. S. 2014. miRNA dysregulation in cancer: towards a mechanistic understanding. Frontiers in genetics 5: 54.

Pang, X., Hogan, E. M., Casserly, A., Gao, G., Gardner, P. D. & Tapper, A. R. 2014. Dicer expression is essential for adult midbrain DA neuron maintenance and survival. Molecular and cellular neurosciences 58: 22–28.

Papapetropoulos, S., Adi, N., Ellul, J., Argyriou, A. A. & Chroni, E. 2007. A prospective study of familial versus sporadic Parkinson's disease. Neuro-degenerative diseases 4 (6): 424–427.

Pasquinelli, A. E., Reinhart, B. J., Slack, F., Martindale, M. Q., Kuroda, M. I., Maller, B., Hayward, D. C., Ball, E. E., Degnan, B., Müller, P., Spring, J., Srinivasan, A., Fishman, M., Finnerty, J., Corbo, J., Levine, M., Leahy, P., Davidson, E. & Ruvkun, G. 2000. Conservation of the sequence and temporal expression of let-7 heterochronic regulatory RNA. Nature 408 (6808): 86–89.

Paul, P., Chakraborty, A., Sarkar, D., Langthasa, M., Rahman, M., Bari, M., Singha, S., Kumar, A., Malakar, A.K. & Chakraborty, S. 2018. Interplay between miRNAs and human diseases. Journal of Cellular Physiology 233 (3): 2007.

Peng, C., Li, N., Ng, Y. K., Zhang, J., Meier, F., Theis, F. J., Merkenschlager, M., Chen, W., Wurst, W. & Prakash, N. 2012. A unilateral negative feedback loop between miR-200 microRNAs and Sox2/E2F3 controls neural progenitor cell-cycle exit and differentiation. The Journal of neuroscience: the official journal of the Society for Neuroscience 32 (38): 13292–13308.

Poewe, W., Seppi, K., Tanner, C. M., Halliday, G. M., Brundin, P., Volkmann, J., Schrag, A. E. & Lang, A. E. 2017. Parkinson disease. Nature reviews. Disease primers 3: 17013.

Polymeropoulos, M. H., Lavedan, C., Leroy, E., Ide, S. E., Dehejia, A., Dutra, A., Pike, B., Root, H., Rubenstein, J., Boyer, R., Stenroos, E. S., Chandrasekharappa, S., Athanassiadou, A., Papapetropoulos, T., Johnson, W. G., Lazzarini, A. M., Duvoisin, R. C., Di Iorio, G., Golbe, L. I. & Nussbaum, R. L. 1997. Mutation in the alpha-synuclein gene identified in families with Parkinson's disease. Science 276 (5321): 2045–2047.

Prajapati, P., Sripada, L., Singh, K., Bhatelia, K., Singh, R. & Singh, R. 2015. TNF-α regulates miRNA targeting mitochondrial complex-I and induces cell death in DA cells. Biochimica et biophysica acta 1852 (3): 451–461.

Provost, P., Dishart, D., Doucet, J., Frendewey, D., Samuelsson, B. & Rådmark, O. 2002. Ribonuclease activity and RNA binding of recombinant human Dicer. EMBO Journal 21 (21): 5864-5874.

Radhakrishnan, B. & Alwin, P. A. A. 2016. Role of miRNA-9 in Brain Development. Journal of experimental neuroscience 10: 101–120.

Ransohoff, R.M. 2016. How neuroinflammation contributes to neurodegeneration. Science 353: 777–83.

Reinhart, B. J., Slack, F. J., Basson, M., Pasquinelli, A. E., Bettinger, J. C., Rougvie, A. E., Horvitz, H.R. & Ruvkun, G. 2000. The 21-nucleotide let-7 RNA regulates developmental timing in *Caenorhabditis elegans* Nature 403 (6772): 901-906.

Riederer, P. & Wuketich, S. 1976. Time course of nigrostriatal degeneration in parkinson's disease. Journal of Neural Transmission 38 (3): 277-301.

Rodriguez, M., Rodriguez-Sabate, C., Morales, I., Sanchez, A. & Sabate, M. 2015. Parkinson's disease as a result of aging. Aging Cell 14 (3): 293-308.

Roser, A. E., Caldi Gomes, L., Schünemann, J., Maass, F. & Lingor, P. 2018. Circulating miRNAs as Diagnostic Biomarkers for Parkinson's Disease. Frontiers in neuroscience 12: 625.

Rupaimoole, R. & Slack, F. J. 2017. MicroRNA therapeutics: towards a new era for the management of cancer and other diseases. Nature reviews. Drug discovery 16 (3): 203–222.

Sanders, A. R., Göring, H. H., Duan, J., Drigalenko, E. I., Moy, W., Freda, J., He, D., Shi, J., MGS & Gejman, P. V. 2013. Transcriptome study of differential expression in schizophrenia. Human molecular genetics 22 (24): 5001–5014.

Sauer, B. 1998. Inducible gene targeting in mice using the Cre/lox system. Methods 14 (4): 381-392.

Sauer, B. & Henderson, N. 1988. Site-specific DNA recombination in mammalian cells by the Cre recombinase of bacteriophage P1. Proceedings of the National Academy of Sciences of the United States of America 85 (14): 5166–5170.

Saurat, N., Andersson, T., Vasistha, N. A., Molnár, Z. & Livesey, F. J. 2013. Dicer is required for neural stem cell multipotency and lineage progression during cerebral cortex development. Neural development 8: 14.

Schrag, A., Jahanshahi, M. & Quinn, N. 2000. How does Parkinson's disease affect quality of life? A comparison with quality of life in the general population. Movement Disorder 15: 1112–1118.

Schaefer, A., O'Carroll, D., Tan, C. L., Hillman, D., Sugimori, M., Llinas, R. & Greengard, P. 2007. Cerebellar neurodegeneration in the absence of microRNAs. The Journal of Cell Biology 178 (2): i5.

Segura-Aguilar, J., Paris, I., Muñoz, P., Ferrari, E., Zecca, L. & Zucca, F. A. 2014. Protective and toxic roles of dopamine in Parkinson's disease. Journal of neurochemistry 129 (6): 898–915.

Selbach, M., Schwanhäusser, B., Thierfelder, N., Fang, Z., Khanin, R. & Rajewsky, N. 2008. Widespread changes in protein synthesis induced by microRNAs. Nature 455 (7209): 58.

Serafin, A., Foco, L., Zanigni, S., Blankenburg, H., Picard, A., Zanon, A., Giannini, G., Pichler, I., Facheris, M. F., Cortelli, P., Pramstaller, P. P., Hicks, A. A., Domingues, F. S. & Schwienbacher, C. 2015. Overexpression of blood microRNAs 103a, 30b, and 29a in L-dopa-treated patients with PD. Neurology 84(7): 645–653.

Sethi, P. & Lukiw, W. J. 2009. Micro-RNA abundance and stability in human brain: specific alterations in Alzheimer's disease temporal lobe neocortex. Neuroscience letters 459 (2): 100–104.

Shabalina, S. A. & Koonin, E. V. 2008. Origins and evolution of eukaryotic RNA interference. Trends in ecology & evolution 23 (10): 578–587.

Sherrard, R., Luehr, S., Holzkamp, H., McJunkin, K., Memar N. & Conradt B. 2017. miRNAs cooperate in apoptosis regulation during c. Elegans development. Genes & development 31: 209–222.

Shih, L. C. & Tarsy, D. 2007. Deep brain stimulation for the treatment of atypical parkinsonism. Movement disorders: official journal of the Movement Disorder Society 22 (15): 2149–2155.

Simunovic, F., Yi, M., Wang, Y., Stephens, R. & Sonntag, K. C. 2010. Evidence for gender-specific transcriptional profiles of nigral dopamine neurons in Parkinson disease. PloS one 5 (1): e8856.

Sinnayah, P., Lindley, T. E., Staber, P. D., Davidson, B. L., Cassell, M. D. & Davisson, R. L. 2004. Targeted viral delivery of Cre recombinase induces conditional gene deletion in cardiovascular circuits of the mouse brain. Physiological genomics 18 (1): 25–32.

Slack, F. J., Basson, M., Liu, Z., Ambros, V., Horvitz, H. & Ruvkun, G. 2000. The lin-41 RBCC Gene Acts in the C. elegans Heterochronic Pathway between the let-7 Regulatory RNA and the LIN-29 Transcription Factor. Molecular Cell 5 (4): 659-669.

Slota, J. A. & Booth, S. A. 2019. MicroRNAs in Neuroinflammation: Implications in Disease Pathogenesis, Biomarker Discovery and Therapeutic Applications. Non-coding RNA 5 (2): 35.

Smirnova, L., Gräfe, A., Seiler, A., Schumacher, S., Nitsch, R. & Wulczyn, F. G. 2005. Regulation of miRNA expression during neural cell specification. The European journal of neuroscience 21(6): 1469–1477.

Song, M. S. & Rossi, J. J. 2017 Molecular mechanisms of Dicer: endonuclease and enzymatic activity. The Biochemical journal 474 (10): 1603–1618.

Spillantini, M.G., Schmidt, M.L., Lee, V.M., Trojanowski, J.Q., Jakes,R. & Goedert, M. 1997. Alpha-synuclein in Lewy bodies. Nature 388: 839-840.

Sternberg, N., Sauer, B., Hoess, R. & Abremski K. 1986. Bacteriophage P1 cre gene and its regulatory region. Evidence for multiple promoters and for regulation by DNA methylation. Journal of Molecular Biology 187 (2): 197-212.

Sternberg, N. & Hamilton, D. 1981. Bacteriophage P1 site-specific recombination. I. Recombination between loxP sites. Journal of Molecular Biology 150 (4): 467-486.

Suárez, Y., Fernández-Hernando, C., Yu, J., Gerber, S. A., Harrison, K. D., Pober, J. S., Iruela-Arispe, M. L., Merkenschlager, M. & Sessa, W. C. 2008. Dicer-dependent endothelial microRNAs are necessary for postnatal angiogenesis. Proceedings of the National Academy of Sciences of the United States of America 105(37): 14082–14087.

Sulzer, D. 2007. Multiple hit hypotheses for dopamine neuron loss in Parkinson's disease. Trends in Neurosciences 30: 244–250.

Surmeier, D. J., Obeso, J. A. & Halliday, G. M. 2017. Selective neuronal vulnerability in Parkinson disease. Nature reviews. Neuroscience 18 (2): 101–113.

Svobodova, E., Kubikova, J. & Svoboda, P. 2016. Production of small RNAs by mammalian Dicer. *Pflügers Archiv - European Journal of Physiology 46*8: 1089–1102.

Tapias, V., Hu, X., Luk, K. C., Sanders, L. H., Lee, V. M. & Greenamyre, J. T. 2017. Synthetic alpha-synuclein fibrils cause mitochondrial impairment and selective dopamine neurodegeneration in part via iNOS-mediated nitric oxide production. Cellular and molecular life sciences: CMLS, 74 (15): 2851–2874.

Thatcher, E. J., Bond, J., Paydar, I. & Patton, J. G. 2008. Genomic organization of zebrafish microRNAs. BMC genomics 9: 253.

Tsien, J. Z., Chen, D. F., Gerber, D., Tom, C., Mercer, E. H., Anderson, D. J., Mayford, M., Kandel, E. R. & Tonegawa, S. 1996. Subregion- and cell type-restricted gene knockout in mouse brain. Cell 87 (7): 1317–1326.

Tufekci, K.U., Oner, M.G. & Meuwissen, R.L. 2014. Genc S. The role of microRNAs in human diseases. Methods of Molecular Biology 1107: 33–50.

Uhlmann, S., Mannsperger, H., Zhang, J. D., Horvat, E. Á., Schmidt, C., Küblbeck, M., Henjes, F., Ward, A., Tschulena, U., Zweig, K., Korf, U., Wiemann, S. & Sahin, O. 2012. Global microRNA level regulation of EGFR-driven cell-cycle protein network in breast cancer. Molecular systems biology 8: 570.

United Nations, Department of Economic and Social Affairs, Population Division. World Population Prospects: The 2015 Revision, Key Findings and Advance Tables. Available online: https://esa.un.org/unpd/wpp/publications/files/key_findings_wpp_2015.pdf. Published on 2015, last accessed on 1.6.2020.

van Heesbeen, H.J. & Smidt, M.P. 2019. Entanglement of Genetics and Epigenetics in Parkinson's Disease. Frontiers in neuroscience 13: 277.

Volpicelli-Daley, L. A., Luk, K. C. & Lee, V. M. 2014. Addition of exogenous α-synuclein preformed fibrils to primary neuronal cultures to seed recruitment of endogenous α-synuclein to Lewy body and Lewy neurite-like aggregates. Nature protocols 9 (9): 2135–2146.

Volpicelli-Daley, L. A., Luk, K. C., Patel, T. P., Tanik, S. A., Riddle, D. M., Stieber, A., Meaney, D. F., Trojanowski, J. Q. & Lee, V. M. 2011. Exogenous α-synuclein fibrils induce Lewy body pathology leading to synaptic dysfunction and neuron death. Neuron 72 (1): 57–71.

Wang, Z. H., Zhang, J. L., Duan, Y. L., Zhang, Q. S., Li, G. F. & Zheng, D. L. 2015. MicroRNA-214 participates in the neuroprotective effect of Resveratrol via inhibiting α-synuclein expression in MPTP-induced Parkinson's disease mouse. Biomedicine & pharmacotherapy = Biomedecine & pharmacotherapie 74: 252–256.

Wang, J., Chen, J. & Sen, S. 2016a. MicroRNA as Biomarkers and Diagnostics. Journal of Cell Physiology 231: 25–30.

Wang, Y., Luo, J., Zhang, H. & Lu, J. 2016b. MicroRNAs in the same clusters evolve to coordinately regulate functionally related genes. Molecular Biology and Evolution 33: 2232–2247.

Wanisch, K., Kovac, S. & Schorge, S. 2013. Tackling obstacles for gene therapy targeting neurons: disrupting perineural nets with hyaluronidase improves transduction. PloS one 8(1): e53269.

Warner, T. T. & Schapira, A. H. 2003. Genetic and environmental factors in the cause of Parkinson's disease. Annals of neurology 53 Suppl 3: S16–S25.

Weber, J. A., Baxter, D. H., Zhang, S., Huang, D. Y., Huang, K. H., Lee, M. J., Galas, D. J. & Wang, K. 2010. The microRNA spectrum in 12 body fluids. Clinical chemistry 56 (11): 1733–1741.

Weinberg, D. E., Nakanishi, K., Patel, D. J. & Bartel, D. P. 2011. The inside-out mechanism of Dicers from budding yeasts. Cell 146: 262–276.

Wienholds, E., Koudijs, M. J., van Eeden, F. J., Cuppen, E. & Plasterk, R. H. 2003. The microRNA-producing enzyme Dicer1 is essential for zebrafish development. Nature genetics 35 (3): 217–218.

Wightman, B., Ha, I. & Ruvkun, G. 1993. Posttranscriptional regulation of the heterochronic gene lin-14 by lin-4 mediates temporal pattern formation in C. elegans. Cell 75 (5): 855-862.

Wingo, A.P., Almli, L.M., Stevens, J.S., Klengel, T., Uddin, M., Li, Y. & Ressler, K.J. 2015. DICER1 and microRNA regulation in post-traumatic stress disorder with comorbid depression. Nature Communications 6: 10106.

Yi, R., Qin, Y., Macara, I. G. & Cullen, B. R. 2003. Exportin-5 mediates the nuclear export of pre-microRNAs and short hairpin RNAs. Genes & development 17 (24): 3011–3016.

Zhang, C. 2008. MicroRNAs: role in cardiovascular biology and disease. Clinical science 114 (12): 699–706.

Zhang, Z. & Cheng, Y. 2014. miR-16-1 promotes the aberrant alpha-synuclein accumulation in parkinson disease via targeting heat shock protein 70. The Scientific World Journal 2014: 938348.

Zhao, L. & Wang, Z. 2019. MicroRNAs: Game Changers in the Regulation of α-Synuclein in Parkinson's Disease. Parkinson's disease 2019: 1743183.

Zheng, K., Li, H., Zhu, Y., Zhu, Q. & Qiu, M. 2010. MicroRNAs are essential for the developmental switch from neurogenesis to gliogenesis in the developing spinal cord. The Journal of neuroscience: the official journal of the Society for Neuroscience 30 (24): 8245–8250.

Zhuang, X., Masson, J., Gingrich, J. A., Rayport, S. & Hen, R. 2005. Targeted gene expression in dopamine and serotonin neurons of the mouse brain. Journal of neuroscience methods 143 (1): 27–32.

Zindy, F., Lee, Y., Kawauchi, D., Ayrault, O., Merzoug, L. B., Li, Y., McKinnon, P. J. & Roussel, M. F. 2015. Dicer Is Required for Normal Cerebellar Development and to Restrain Medulloblastoma Formation. PloS one 10 (6): e0129642.